Institute of Chemical Research of Catalonia

UNIVERSITAT ROVIRA i VIRGILI

Azobenzene derived cyclic carbonate monomers for ring-opening polymerization: Towards photo-responsive polymers.

Master's degree in Synthesis, Catalysis and Molecular design

2024-2025

Tarragona

Ward Adrianus Cornelis Gerardus Vermeer

Supervised by Prof. Arjan W. Kleij and Dr. José A. Berrocal.

Index

1. Abbreviations and acronyms

T_d^5	Thermal degradation 5%	KO^tBu	Potassium *tert*-butoxide
UV	Ultraviolet.	*n*BuLi	*n*-butyllithium
ICIQ	Institut Català d'Investigació Química.	EDC	1-ethyl-3-(3-dimethylaminopropyl)carbodiimide
Dr.	Doctor.	DIPEA	Di-isopropylethylamine
Prof.	Professor.	MEK	Methyl Ethyl Ketone
PC	Polycarbonate	nm	nanometer
ROP	Ring-opening polymerization	Sn2	Bimolecular Nucleophilic Substitution
T_g	Glass transition temperature	DCU	dicyclohexylurea
Đ	Dispersity	DMAP	4-dimethylaminopyridine
TBD	Triazabicyclodecene	$(HCHO)_n$	Polymerized formaldehyde
CO_2	carbon dioxide	EDU	Dimethylaminopropyl (urea)
E	Entgegen (opposite)	M_n	number average molecular weight
Z	Zusammen (together)	TBAI	Tetra-*n*-butylammonium iodide
r.t.	Room temperature	DMSO	Dimethyl sulfoxide
HRMS	High Resolution Mass Spectrometry	ESI-MS	Electrospray Ionization Mass Spectrometry
DCC	dicyclohexylcarbodiimide	DSC	Differential Scanning Calorimetry
TGA	Thermogravimetric analysis	SEC	Size Exclusion Chromatography
ln	Natural logarithm	*m*CPBA	meta-Chloroperoxybenzoic acid
BnOH	Benzyl alcohol	UV-VIS	Ultraviolet-Visible Spectroscopy
TMS	tetramethylsilane	NMR	Nuclear Magnetic Resonance
DMF	dimethylformamide	ABS	absorbance
THF	tetrahydrofuran	TLC	thin-layer chromatography
°C	degrees Celsius		

2. Abstract

Azobenzene is well known for its photo-responsive behavior. Upon UV irradiation, the molecule undergoes isomerization from *trans* (or: *E*) to *cis* (or: *Z*). Such an isomerization in macromolecules functionalized with azobenzene fragments can lead to multiple changes in the compound's properties, like melting temperature or glass transition. As a result, a polymeric molecule could undergo a solid-to-liquid transition upon irradiation, enabling (for instance) better processability.

Polycarbonate macromolecules are thermoplastic polymers that can be made, among other methods, through the ring-opening polymerization (ROP) of cyclic carbonates. Polycarbonates have a wide range of applications, including their use in construction materials and as additives in the automotive industry, electronics and 3D printing.

The main objective of my master project is to equip cyclic carbonate monomers with an azobenzene moiety and evaluate this monomer towards anionic ROP. I will focus on azobenzene fragments that can be introduced in the polymer architecture, and the molecular weight (M_n) and dispersity ($Đ$) of the synthesized polymers. Furthermore, attempts will be made to photo-isomerize the azobenzene units in the envisioned polycarbonate with the aim of inducing reversible changes of its thermal and mechanical behavior, which will be studied by DSC, TGA, NMR, and UV-vis spectroscopy.

Both targeted monomers **M1** and **M2** were successfully synthesized, and their ROP was carried out by anionic ring-opening polymerization, using benzyl alcohol (as initiator) and TBD as catalyst affording polymer 1 (**P1**) and polymer 2 (**P2**). **P1** was obtained, after optimization, with a molecular weight of 3.51 kg/mol and a $Đ$ of 1.2. **P2** was obtained with a molecular weight of 2.29 kg/mol and a $Đ$ of 1.4. Both polymers were irradiated with UV light, and the photo-responsive azobenzene was successfully isomerized from *cis* to *trans*. Kinetic studies for the relaxation after isomerization of the azobenzene moiety were done and confirmed a 1st order kinetic process. Unfortunately, no T_g change was observed after irradiation. Therefore, further modification of the polymer design may reveal more possibilities for a thermal transition. Nevertheless, the synthesized photo-responsive polycarbonate polymers provide insight into the design of stimuli-responsive materials and lay a solid foundation for future research in this field.

3. Introduction and theoretical background

This master's thesis was developed at the Institut Català d'Investigació Química (ICIQ) in the research groups of Prof. Arjan W. Kleij and Dr. José A. Berrocal. The group of Prof. Arjan W. Kleij has extensive expertise in the field of cyclic carbonates, while photochemical switching is well-studied in the group of Dr. José A. Berrocal. By combining the expertise of both groups, this work aims to advance the synthesis and study of photo-responsive biobased carbonate polymers.

3.1 General

Increasing levels of carbon dioxide (CO_2) have been a harsh reality for many years and represent an environmental challenge for modern society. Greenhouse gas emissions cause global warming and the melting of ice. This is caused not only by CO_2 emissions, but also by other gases like methane, nitrous oxide, ozone, and water vapor (Figure 1). This significant increase in CO_2 emissions is primarily driven by the combustion of fossil fuels for energy production, agricultural activities, and the deliberate clearing of forested areas[1]. The biggest rise in global carbon emissions occurred in the *Industrial Revolution*. The extensive use of coal and oil for the production of energy and steel (and to a much lesser extent for chemical production) has led to a substantial increase in anthropogenic CO_2 emissions[2].

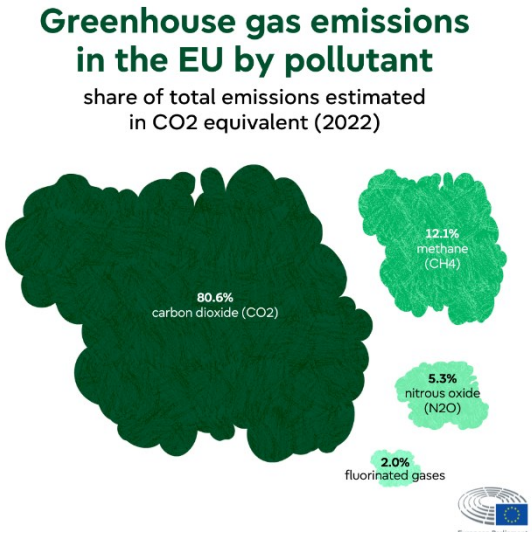

Figure 1 Greenhouse gas emissions in the EU by pollutant. Source: European Environment Agency.

In the 20th century, the increase in CO_2 emissions did not stop. Energy production transitioned from coal and oil to less polluting petroleum sources. However, an increase in CO_2 emissions still occurs today. By the end of the 20th century, CO_2 emissions broke all former records known in human history. This trend is still continuing in this century, and will likely not decrease if proper countermeasures are taken. The current increase in carbon emissions cause immense concerns about the future of the planet and humankind. One of the many causes of this increase is the production of cement[3]. CO_2 is one of the byproducts

during the production of cement, and it is formed during the chemical reaction between limestone and clay.

The planet plays a big role in keeping a controllable carbon balance (known as the carbon cycle), capturing CO_2 and regulating the concentration in the atmosphere. Earth does this by photosynthesis, and large amounts of CO_2 are absorbed this way by the planet through forests and oceans[4]. Their combined effects have preserved our ecosystems for millions of years. Unfortunately, because of human-caused emissions of CO_2, this carbon cycle is out of balance. This imbalance and disruption are linked to climate change and global warming. This causes a significant effect on various ecosystems, natural processes, weather patterns, the melting of polar ice and rising sea levels[5].

Because of this carbon imbalance, human intervention is necessary to prevent further escalation. A key strategy is to implement the large-scale use of sustainable energy into day-to-day life. Using fewer fossil fuels and being more efficient with their consumption is highly important. Humankind can also contribute by leveraging scientific knowledge and innovation to reduce CO_2 emissions and help to restore the atmospheric carbon balance. CO_2 capture is a potential solution to restore the balance of this problem. Among promising approaches, CO_2 capture has been a widely investigated area in recent years. Techniques such as membrane-based separation allow for the selective capture of the CO_2 from the air. In the chemical industry, considerable efforts have been made towards CO_2 capture. In several cases, CO_2 has been incorporated into new carbon-based compounds and the formation of useful carbon-based synthetic intermediates[6–9]. This has a double positive impact, combining the reduction of CO_2 from the air and the reduction of greenhouse gases. An example of this is the formation of cyclic carbonates via CO_2 insertion into cyclic ethers. This showcases the potential of CO_2 as an effective building block in the synthesis of new carbon-based structures, such as cyclic carbonates[10].

3.2 Polycarbonates

Among the diverse range of known sustainable polymers, aliphatic polycarbonates stand out due to their unique chemical structure and promising environmental profile. Defined by the presence of carbonate groups [–O–(C=O)–O–] in their main chain, these polymers are not only biocompatible and biodegradable, but can also be derived from renewable resources[11]. Polycarbonates are particularly attractive as the presence of the carbonate moiety and the absence of acidic functional groups contribute to an enhanced stability in

comparison to polyesters, often regarded as leading materials in the field of polymers. Indeed, the degradation rate of polycarbonates is significantly slower than that of polyesters[12]. The overall combination of beneficial properties and environmental compatibility has led to an increase in the use of polycarbonates, highlighting their strong potential for a wide range of applications.

Polycarbonates are well-known for their potential in environmental and biomedical industries. Due to their weak flammability, biodegradability, and biocompatibility they have been used for various biomedical uses are listed below:

- Drug delivery represents a significant application area for polycarbonates. These polymers are used across various industries, including agrochemical, veterinary, and medical fields. Drug molecules can be chemically bound to the polymer backbone, allowing for controlled release at targeted sites due to the polymer's biodegradable properties[13].
- Biodegradable polymers have been evaluated for toxicity and proven to be cytocompatible, and they offer potential in medical applications. They can serve as alternatives to the presence of metals in biomedical implants, such as plates, clips, and bone pins, providing temporary support while degrading within the body over time[14].

Synthesis of polycarbonates is a well-established area of research in the Kleij group. In addition, the design of novel cyclic carbonates has been a main interest of the group for many years. The group has also contributed significantly to the development of biobased polycarbonates. The requisite biobased carbonate monomers are normally synthesized by the incorporation of CO_2 into the molecule. To facilitate these reactions, the group developed an aluminum catalyst (Figure 5)[15,16].

Cyclic carbonates can be used in ring-opening polymerization (ROP) to afford polycarbonates. Ring-opening polymerization can proceed via different mechanisms, with the initiation occurring via anionic, cationic, and coordination-insertion type mechanisms[17–19]. Among these, anionic ROP is the predominant technique used by the Kleij group. In anionic ROP, six and seven-membered cycles are commonly used due to the favorable thermodynamics involved, allowing smooth polymerization. 5-Membered cycles, however, are thermodynamically more stable, and only rare examples exist for their ROP.

The use of appropriate solvents can influence this polymerization process, and the most common solvents are tetrahydrofuran (THF), toluene, and dimethylformamide (DMF).

Mechanistic aspects of the anionic ring-opening polymerization are well known (Scheme 1). The initiation of the polymerization occurs by nucleophilic attack of the initiator at the electrophilic carbonate moiety. A commonly used initiator is benzyl alcohol (BnOH). After initiation, an alkoxide anion is (repeatedly) generated, which acts as the active species in the polymerization. The alkoxide attacks subsequent carbonate monomers, and chain-growth polymerization occurs. The chain-growth reaction will continue until full conversion of the monomer is achieved, but can also be terminated by the addition of an acid such as HCl or HOAc.

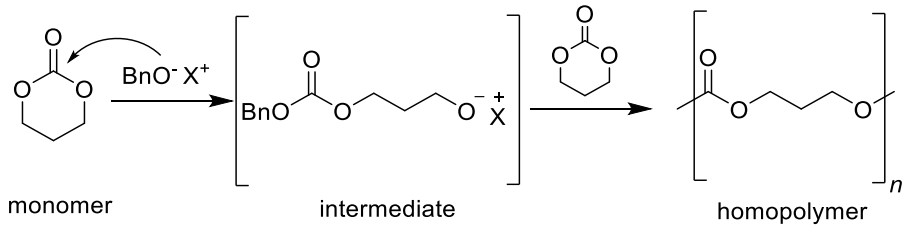

Scheme 1 Anionic ring-opening polymerization mechanism of cyclic carbonates.

Various catalysts can be used to facilitate ROP, including Brønsted bases, metal catalysts, Brønsted acids and enzymes. Among Brønsted bases, many classes are effective, including guanidines, amidines, tertiary amines, *N*-heterocyclic carbenes and thiourea-based tertiary amines[20]. In our group, mainly the Brønsted base triazabicyclodecene (TBD) has been employed. TBD functions as a unique catalyst due to its dual hydrogen-bond donor and acceptor properties. This dual function enables the activation of the ring-opening polymerization by simultaneously activating the incoming nucleophile (BnOH) and the carbonate ring, with TBD facilitating the reaction through a proton-relay sequence. For these reasons, TBD is used as the catalyst in this master's project[21].

3.3 Azobenzene

Azobenzene is well known for its ability to undergo photoisomerization, making it a key compound in the development of photo-responsive materials (Scheme 2). These compounds have been studied since 1937[22]. Structural modification, such as introducing substituents such as a(n) halide, aryl, alkyl, ester and carboxylic acid at different ring positions can significantly influence the photochemical and physical properties of the azobenzene derivatives. In its thermodynamically most stable form (*trans*), it exhibits a strong absorption band in the UV region (325 nm) corresponding to a π-π* transition, and a weaker absorption band (n-π*) in the visible light range (440 nm). Upon exposure to UV light (365 nm) the molecule undergoes isomerization to its *cis*-isomer, which absorbs in the visible light region more strongly for the n-π* transition. Although the maximum absorption of the azobenzene used in this project is at 325 nm, azobenzene exhibits a broad absorption range. Therefore, irradiation at 365 nm is still effective for inducing the photo-responsive behavior of the azobenzene moieties. The reverse isomerization from *cis* to *trans* can occur either via thermal relaxation or upon irradiation with visible light (400-450 nm). Depending on the stability of the *cis* isomer, the half-life of this isomer can vary. The relaxation to the *trans* form can take hours or even days in some cases, depending on the substituents on the azobenzene rings[23,24].

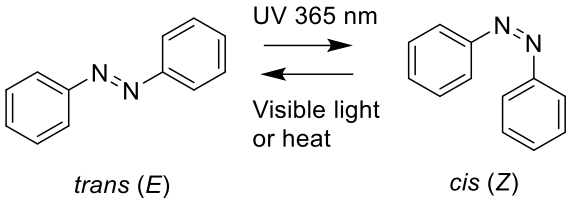

Scheme 2 Azobenzene cis-trans photo-isomerization.

This photoisomerization of *trans* to *cis* azobenzene may induce changes in the polymer, like polarity, crystallinity, stability, melting point, color and other properties. The photoisomerization can cause a solid-to-liquid transition, and crystalline azobenzene compounds may liquefy upon irradiation. In 1937, Hartley observed that the melting point of *cis*-azobenzene (35 °C) was approximately 33 °C lower than that of *trans*-azobenzene (68 °C)[22]. Substituted azobenzenes demonstrate even more pronounced differences in melting behavior. For example, introducing a halogen in the *para* position of one of the aromatic rings results in melting point changes from 82-91 °C (*trans*) to 32-63 °C (*cis*) depending on the specific halogen. Similarly, a *para* "methoxy ester" substituent can decrease the melting point from 125 °C (*trans*) to 65 °C (*cis*). The same holds for a "methoxy" group in *para*, the melting point changes from 54 °C (*trans*) to 25 °C (*cis*)[24,25].

It is important to note that complete conversion from *trans* to *cis* azobenzene is rarely achieved upon irradiation. Instead, a photostationary state is established, in which the *cis*/*trans* ratio depends on the nature and position of substituents on the aromatic rings[26].

3.4 Azobenzene polymers

By combining polycarbonate monomers with azobenzene compounds, it is possible to design and synthesize photo-responsive polymers. In the literature, azobenzene moieties are often embedded into polymeric systems. Various designs can be employed, including introducing azobenzenes in the side-chain, main-chain, crosslinking units and using either dendrimers, hyperbranched polymers and other architectures. Figure 2 provides a visual overview of these different, azobenzene-containing architectures[27]. An example of a polymer with an azobenzene moiety was reported in 1995 by Tripathy, Kumar and coworkers[27]. When they explored the newly prepared material, irradiation by a laser beam isomerizes the azobenzene moieties from *trans* to *cis*. They observed a change in properties, marking the development of the first azobenzene-based photo-responsive polymer.

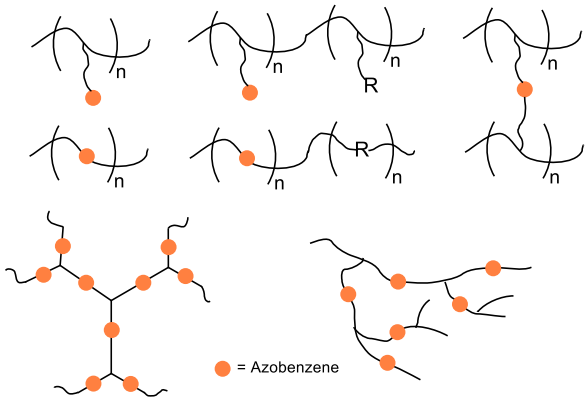

Figure 2 Different architectures of azobenzene photo-responsive polymers. The orange dots illustrate the azobenzene moieties.

In 2007, Wang and coworkers[28] reported a photo-responsive azobenzene-derived block copolymer (Figure 3). The polymer was composed of a poly (acryloyl chloride) backbone that was post-functionalized with an azobenzene containing a hydroxy group. This hydroxy group reacts with an acyl chloride to form an ester bond. When the polymer was exposed to water, colloids were formed. When those colloids were irradiated with UV light, they underwent a shape change from spherical to elliptical, resulting from the isomerization of the azobenzene fragment. Particular relevance to this work is the strategy used for covalent incorporation of azobenzene onto the polymer backbone. This offers a promising route for integrating photo-responsive functionality into polycarbonates.

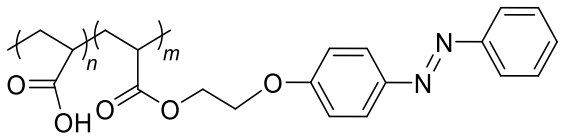

Figure 3 Polyacrylate backbone with a short chain and azobenzene moiety.

One notable study by Hans-Jürgen Butt[29] explored similar polymer architectures. They described a polyacrylate backbone with a flexible spacer of 6 carbons and an azobenzene moiety (see Figure 4). The T_g of the polymer was 48 °C. When the polymer was irradiated with UV light, the T_g dropped to -6 °C. This indicates a solid-to-liquid phase transition upon irradiation. Also, they demonstrated how this solid-to-liquid phase transition can act as a self-healing polymer system. When a polymer film was physically damaged (cracked), it was possible to irradiate (UV) the film and liquefy the damaged part. The material softened and flowed into the damaged region. When this part was irradiated with visible light, reverse isomerization occurs, solidifying the polymer and healing the crack.

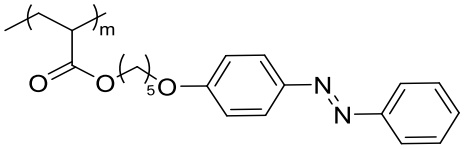

Figure 4 Polyacrylate with a large azobenzene chain.

4. Objectives

As described in the introduction, the combination of biobased cyclic carbonates with photo-responsive azobenzene units has huge potential. Therefore, the **main objective** in this Master's project is to synthesize and study photo-responsive biobased carbonate polymers. To this end, we will approach this challenge by the outline provided below, with a visual summary of the project strategy presented in Scheme 3.

I. **Monomer synthesis:** The synthesis of a bicyclic carbonate as the monomer backbone of the target polymer is carried out through a 3-step synthesis. First, the formation of a hydroxy group onto a cyclohexene starting material. Then, the epoxide formation of the alkene functionality and the carbonate formation via CO_2 insertion. Once the bicyclic carbonate core is synthesized, azobenzene-based photo-responsive units will be attached. Two monomer variants will be synthesized. In monomer 1 (**M1**), the azobenzene is directly attached to the cyclic carbonate base by Steglich esterification. In monomer 2 (**M2**), a 6-carbon spacer will be inserted between the cyclic carbonate and the azobenzene by a multistep synthesis.

II. **Ring-opening polymerization:** After the monomer synthesis, anionic ring-opening polymerization will be employed to form polycarbonates. This step will focus on achieving well-defined polymers while measuring pertinent data such as M_n, $Đ$, T_g, T_d^5, NMR and IR spectroscopic data. Optimization of the process will be attempted by variation of the reaction temperature, time, amount of initiator and catalyst.

III. **Photo-responsive characterization:** After finishing phase II, photo-isomerization will be carried out on the azobenzene units in the envisioned polycarbonate to induce reversible changes in the thermal and mechanical behavior of these macromolecules, which will be studied by DSC, NMR, and UV-vis spectroscopy.

The feasibility of this project comes from the combination of Prof Arjan W. Kleij's knowledge of the ROP of biobased cyclic carbonates with Dr. José Berrocal's expertise in photo-responsive materials and the study of their properties.

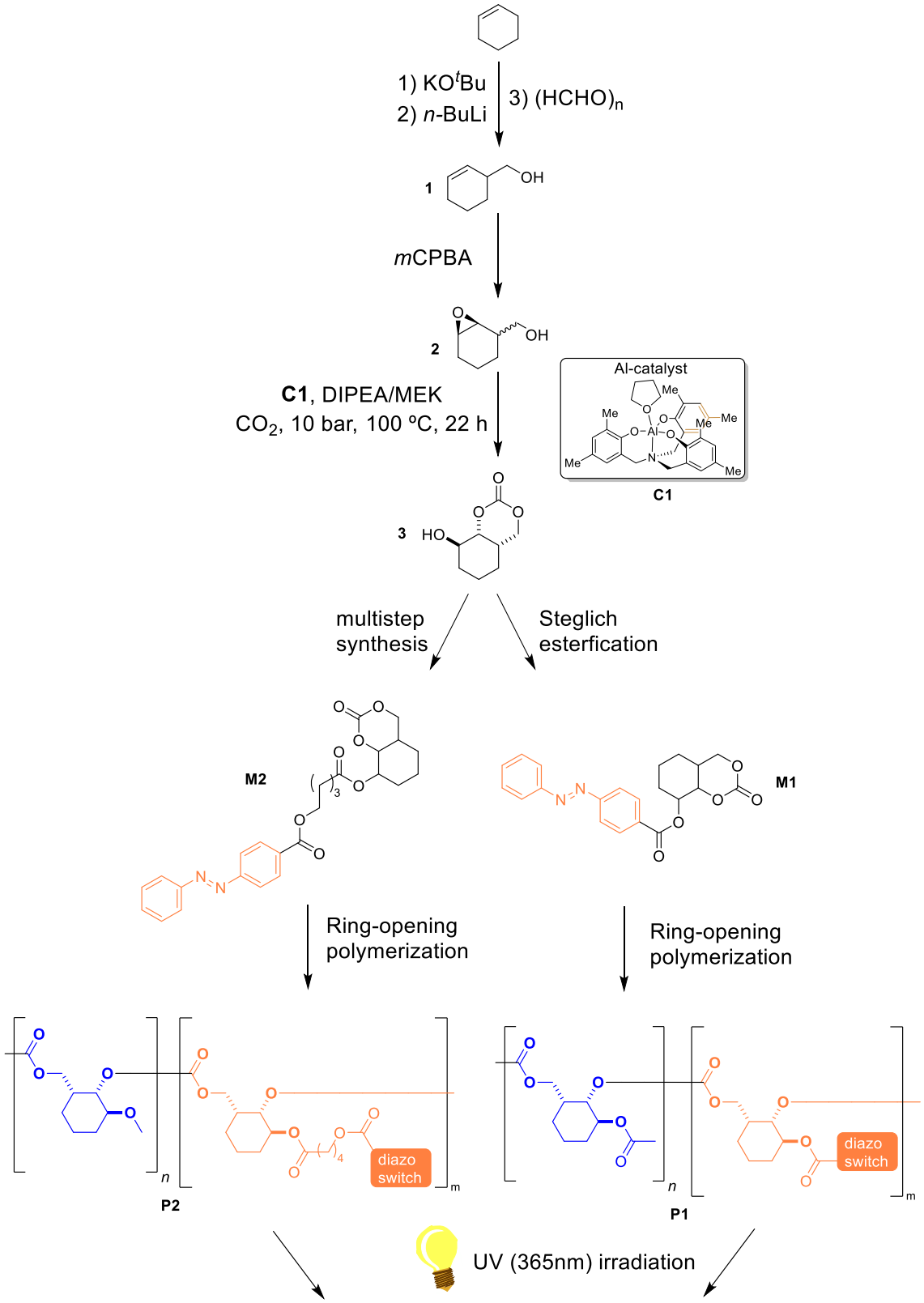

Scheme 3 Outline of this Master's thesis project.

5. Results and discussion

5.1 Synthesis of monomer backbone

The synthesis of the target bicyclic carbonate proved to be particularly challenging and involved several steps. In these steps, selectivity and yield were significant obstacles. The first step is the functionalization of cyclohexene to introduce a hydroxyl group. This was done by using potassium *tert*-butoxide and *n*-butyllithium, which creates a so-called super base. This super base can effectively deprotonate the allylic position of the cyclohexene to create a carbanionic intermediate[30]. Upon treatment with polymerized formaldehyde ($(HCHO)_n$), the carbanionic intermediate reacts to generate the desired hydroxy group. The next step involves the epoxidation of the double bond. This was done with *m*-CPBA (*meta*-chloroperbenzoic acid) in methanol for 16 hours at room temperature. Methanol was used to favor the formation of the *anti*-diastereomer, which is crucial for the subsequent carbonate formation. However, it also introduces complications. Under the acidic conditions of the reaction, methanol (being a nucleophile) can ring-open the epoxide. Such a methanolysis byproduct was isolated, characterized, and thus the potential nucleophilic attack on the epoxide could be confirmed, which unfortunately lowered the overall yield. The amount of *anti*-product was low because it is the thermodynamically less favored product and typical mixtures of 20:80 *anti*:*syn* were obtained. Both diastereoisomers are difficult to separate and, therefore, were used as such in the next step.

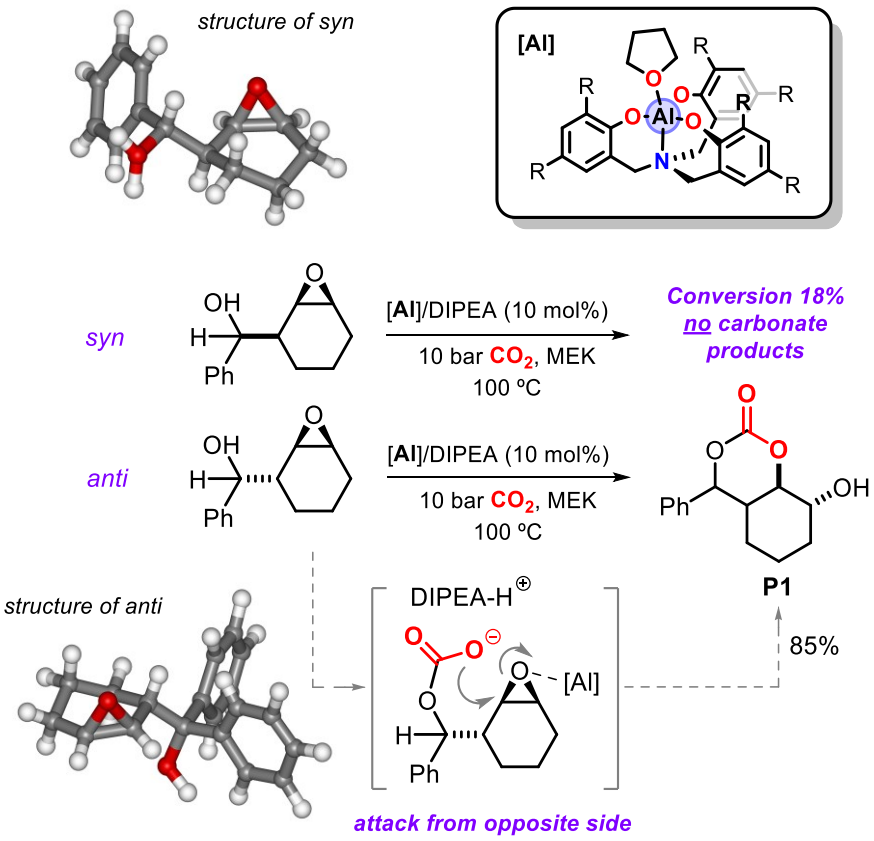

Figure 5 Syn and anti-isomers of the employed bicyclic carbonate structure and their different reactivity.

The final transformation was the formation of the bicyclic carbonate. However, only the *anti*-configured β-epoxy alcohol can undergo intramolecular cyclization with CO_2, to yield a six-membered bicyclic carbonate. The *syn*-isomer, on the other hand, fails to react due to steric constraints and poor alignment for nucleophilic attack, as shown in Figure 5. The *anti*-isomer can undergo proper catalyst activation to favor the nucleophilic attack from the opposite side to induce ring closure. The catalyst used in this transformation is an aluminum-based catalyst developed in the group of Prof. Arjan W. Kleij. This catalyst is well-known for its epoxide activation potential, which increases its electrophilicity. This facilitates the ring-opening of the epoxide and thus the insertion of CO_2[15,16].

5.2 Synthesis of monomer 1 (**M1**)

Once the monomer backbone was successfully synthesized, the remaining hydroxy group could be used to functionalize the carbonate with an azobenzene group. Among the various synthetic possibilities for functionalization, we opted for the Steglich esterification. This is a reliable method for the coupling of an alcohol with a carboxylic acid. In a publication of Kleij et al., these hydroxy-carbonate scaffolds could be coupled to a variety of drug molecules by this method[31]. Building on this precedent, the Steglich esterification emerged as the most suitable reaction for our purpose. *Para*-substituted carboxylic acid azobenzene (**4**, Figure 6) was chosen as a model scaffold for the investigation towards a proof-of-concept photo-responsive polycarbonate. The Steglich esterification was performed under standard conditions, using dicyclohexylcarbodiimide (DCC) and 4-dimethylaminopyridine (DMAP) in dry dichloromethane at room temperature for 4 hours. DCC serves as an effective coupling agent under mild conditions and is especially advantageous for sterically hindered alcohols. One drawback of this method is the formation of dicyclohexylurea (DCU) as a byproduct. DCU is poorly soluble in most organic solvents and often complicates purification. Table 1 shows the various purification attempts made. While the literature suggests that there are several approaches to remove DCU, none were directly applicable to this specific reaction and product. Column chromatography failed to separate the urea byproduct, and precipitation with various solvents was initially unsuccessful. After several attempts, approximately 97% of the DCU could be removed by precipitation using cold ethyl acetate, resulting in a clean product with an isolated yield of 58%.

Table 1 Removal of the DCU byproduct from the Steglich esterification.

Entry	Solvent	DCU removal
1	Hexane:ethyl acetate	0%
2	Dichloromethane	0%
3	Ethyl acetate	0%
4	Diethyl ether	0%
5	Eluent hexane:ethyl acetate	0%
6	*Cold* ethyl acetate	**97%**

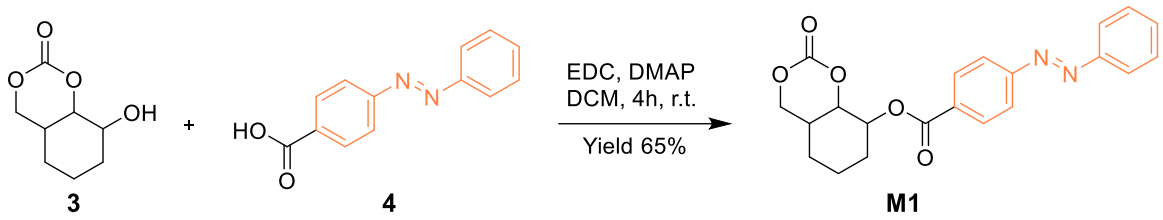

Figure 6 Synthesis of monomer M1 by Steglich esterification.

Eventually, the Steglich esterification with DCC was not productive towards scale up while providing pure enough monomer, and therefore, other approaches were studied[32,33]. The biggest drawback was the urea byproduct, which was difficult to separate from the desired product. As a result, 1-Ethyl-3-(3-dimethylaminopropyl)carbodiimide (EDC, Figure 7), an alternative coupling agent was explored. In contrast to DCC, EDC forms (dimethylaminopropyl)urea (EDU) as a byproduct, which is water-soluble[32,33] and, hence, easily removable by aqueous work-up. The work-up was done by washing 3 times with 2M HCl to protonate the formed EDU. Though the target product **M1** contains an ester group, it remains stable under these acidic conditions, likely because it is sterically protected. To further purify the reaction mixture, $NaHCO_3$ was used 3 times to wash out all the unreacted starting material and brine to remove water residues. This modified method resulted in a cleaner product with a yield of up to 76%. After comparing both methods, the Steglich esterification with EDC as coupling agent proved to be more efficient (Figure 6).

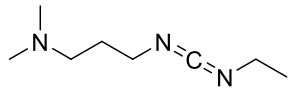

Figure 7 1-Ethyl-3-(3-dimethylaminopropyl)carbodiimide (EDC).

A single crystal suitable for diffraction was successfully grown from a $CDCl_3$ solution inside an NMR tube. The crystal was analyzed by X-ray diffraction (XRD). The determined molecular structure confirmed the proposed atom-connectivity in the product (Figure 8). The crystal structure provided valuable insights into the

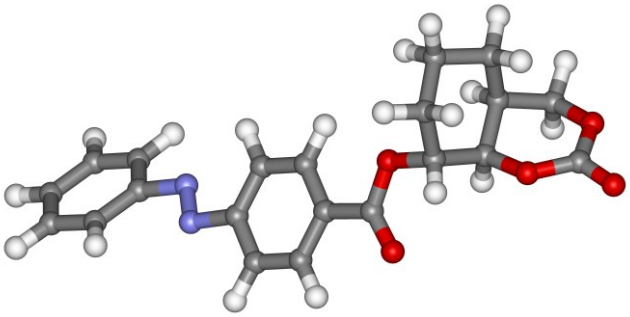

Figure 8. X-ray molecular structure determined for monomer M1.

intermolecular interactions present in the solid state. Interestingly, the monomer does not have direct π-π stacking between the aromatic rings of the azobenzene units. Instead, interactions between the cyclic carbonate scaffolds are observed.

5.2.1 Isomerization studies of Monomer 1

UV-Vis: Figure 9 shows the absorption spectra of **M1** before and after isomerization induced by irradiation. The blue line represents the absorbance prior to irradiation, showing a strong absorption band at 325 nm for *trans*-azobenzene. Upon irradiation for 20 seconds, the absorbance at 325 nm (*trans*) decreases, while the absorbance at 440 nm (predominant light absorption from the *cis* isomer) slightly increases. This shift confirms the isomerization from *trans* to *cis*. Interestingly, no further spectral changes were observed after an additional 20 seconds of irradiation, suggesting that a maximum level of isomerization was achieved within the first irradiation period of 20 seconds[34].

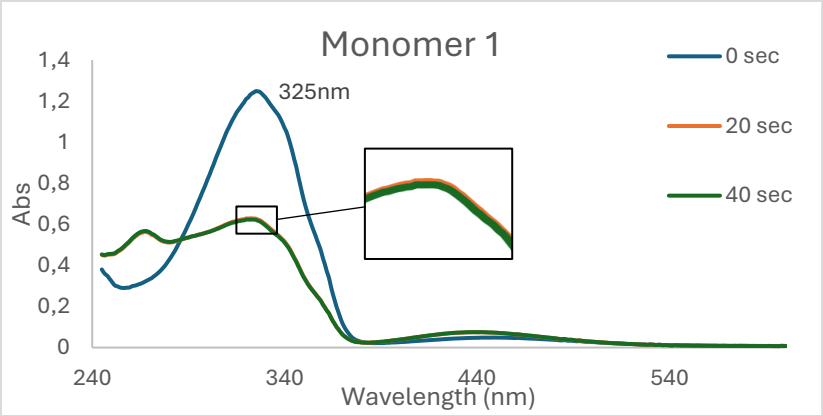

*Figure 9 UV-VIS spectra of **M1**, duration of irradiation for maximum conversion from trans to cis.*

NMR: After synthesizing the monomer, the photo-responsive behavior of the azobenzene moiety attached to the carbonate scaffold was also investigated by NMR[35]. Azobenzene is well-known for undergoing *trans*-to-*cis* isomerization upon irradiation with UV light (365 nm). To further probe this, the monomer was dissolved in dichloromethane and irradiated for 100 seconds with 365 nm light. A visible color change from light yellow to darker yellow was observed. This color change was a first indication that azobenzene successfully isomerizes from *trans* to *cis*. This isomerization was then tracked by ^{1}H-NMR, see Figure 10. Upon irradiation, the characteristic signals of the *trans* monomer (black trace) decreased in intensity, while new peaks corresponding to the *cis* isomer (orange trace) appeared. This

shift in the aromatic region confirms the isomerization of the azobenzene from the *trans* to *cis* configuration by irradiation with UV light. Before irradiation, the mixture contains a 90:10 *trans*:*cis* ratio. After irradiation, a photostationary state was observed, and the ratio between *trans* and *cis* isomers is then approximately 60:40[34,36].

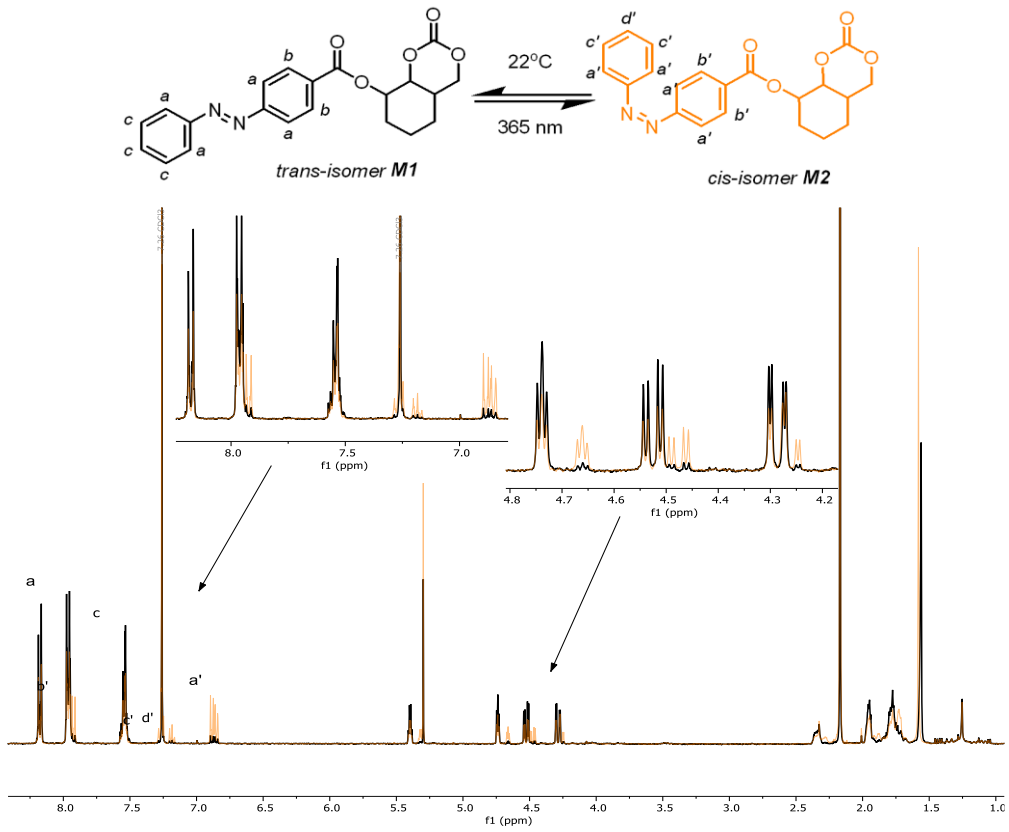

*Figure 10 ^{1}H-NMR spectrum of **M1**, black before irradiation and orange after irradiation with UV light (365nm).*

To investigate the thermal relaxation (22-23 °C) of the *cis* isomer back to the thermodynamically more stable *trans* isomer, ^{1}H-NMR was employed for a time-dependent study over a period of 114 hours[36]. The first spectrum was recorded before irradiation. Upon irradiation, a significant decrease in the *trans* signals was observed, together with the appearance of new signals corresponding to the *cis* isomer. Multiple spectra over multiple days were taken, and the back isomerization from *cis* to *trans* was studied (Figure 11). The ratio between *trans* and *cis* isomers was compared by integration of the *trans* and *cis* peaks in the ^{1}H-NMR spectrum. After 3 days of relaxation, the back isomerization to *trans* has reached a maximum with a *trans*:*cis* ratio of 80:20. In the following days, no further changes were observed, which indicates that the maximum achievable *cis*/*trans* equilibrium state was observed. Before irradiation, the mixture of *trans* and *cis* was 90:10. After irradiation,

the photostationary state was reached and a *trans-cis* ratio of 60:40 was observed[37,38]. The half-life time of the back isomerization of the photo-responsive azobenzene from *cis* to *trans* was calculated. The half-life time of **M1** was $t_{1/2}$ = 0,693/0,00766= 105 hours in normal conditions (stored in the fume hood, not in dark conditions) at 22-23 °C.

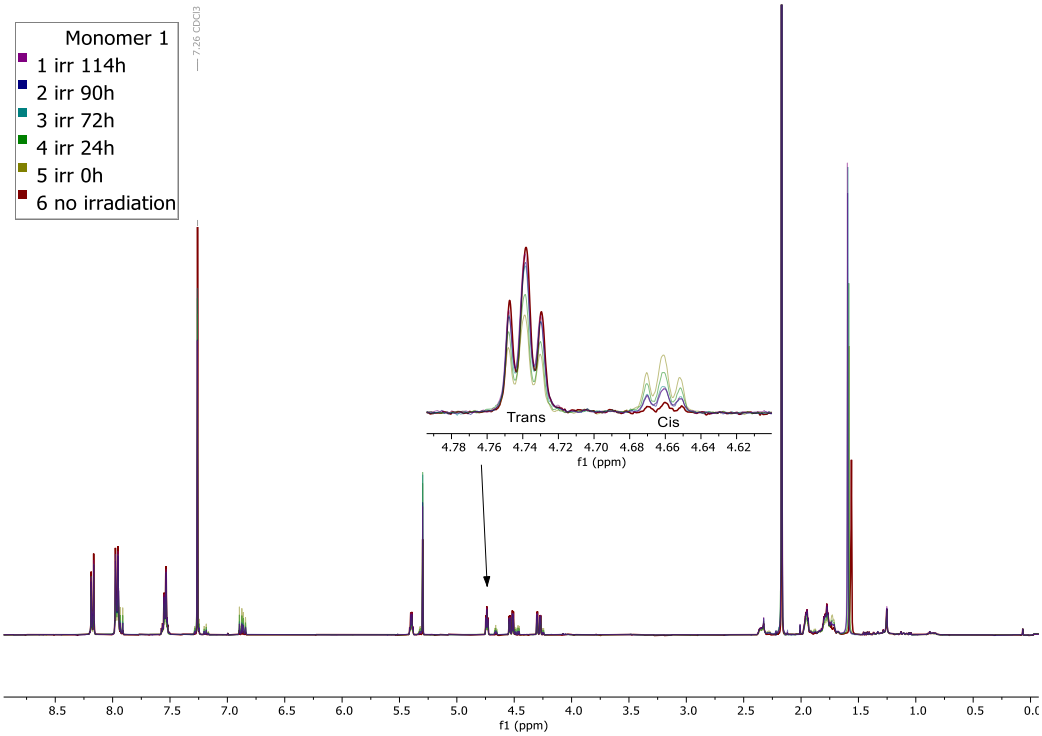

*Figure 11 **M1** relaxation experiment from cis → trans. The insert shows the peaks that were used for comparison.*

Another important feature of azobenzene is its color that changes upon photo-isomerization. When an azobenzene derivative isomerizes from *trans* to *cis*, the absorption of the compound changes. This is caused by the well-known π-π* and n-π* transitions of the *trans* and *cis* isomers. As a result, the compound exhibits a visible color change. Figure 12 illustrates this effect, before and after irradiation, and isomerization[39,40].

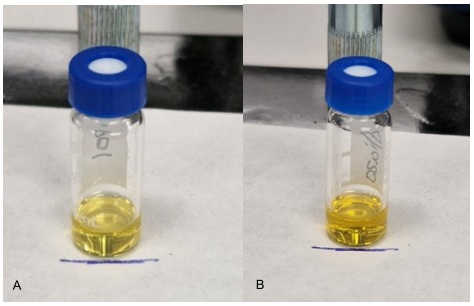

Figure 12 A: before irradiation, B: after irradiation with UV light (365 nm).

5.3 Synthesis of Monomer 2 (**M2**)

In the literature, azobenzene-functionalized polymers typically feature a spacer (usually an alkyl chain) between the photo-responsive azobenzene unit and the polymer backbone[29]. Therefore, the synthesis of such a monomer was next considered. The presence of the alkyl chain increases the molecular flexibility of the azobenzene unit, thereby enhancing its degree of freedom. This structural mobility allows the isomerization to have a more pronounced effect on the properties of the polymer. Furthermore, this approach has been reported in the literature to influence aspects such as the thermal properties[29]. The objective at this stage of development was thus to synthesize a monomer with a carbon-based alkyl spacer between the carbonate and the azobenzene (Scheme 4). After an extensive literature review, it was confirmed that 6-carbon chains are most commonly used to have enough flexibility[29,41,42]. The cyclic carbonate precursor contains a readily functionalizable alcohol group. However, it is relatively laborious to synthesize and sensitive to high temperatures. The synthetic strategy was thus first to attach the alkyl chain to the azobenzene. Subsequently, the functionalized azobenzene is then coupled to the cyclic carbonate.

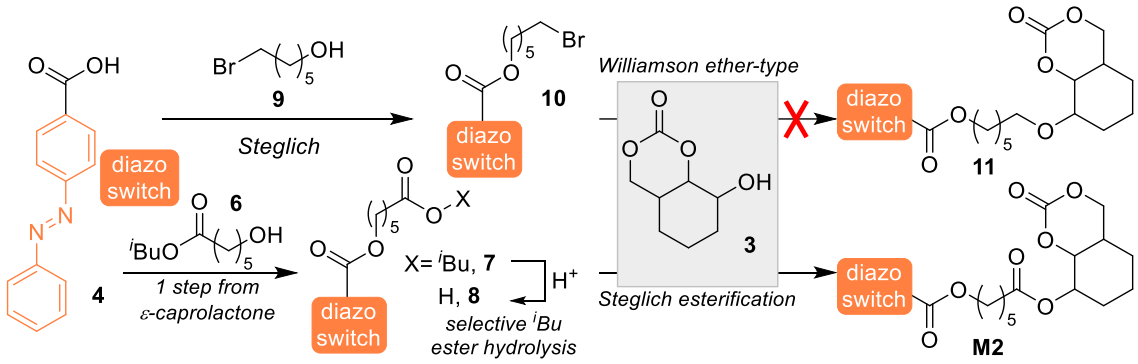

Scheme 4 Overview of the first and second synthetic approach.

In the literature[43], a bifunctional chain containing both an alcohol group and an alkyl bromide (**9**) was reported. The alcohol group in the cyclic carbonate can be easily functionalized by Steglich esterification, while the alkyl bromide enables modification via a Williamson ether synthesis. The first step in this synthetic route involves the coupling of the alkyl chain to the azobenzene moiety. Given the success of the Steglich esterification with EDC towards monomer **M1**, the same strategy for **M2** was adopted[32,33] using similar reactions conditions. The Steglich esterification proceeded successfully, yielding the

desired product (**10**) in good yield (67%). The next step in this approach involves coupling of the chain-functionalized azobenzene and the carbonate moiety.

Table 2 Different conditions probed for the Williamson ether synthesis.

Entry	TBAI	Base	Solvent	Temperature (°C)	Time (h)	Conversion (%)
1	–	K_2CO_3	DMF	r.t.	24	0
2	1 equiv	K_2CO_3	DMSO	50	24	0
3	–	K_2CO_3	Acetone	56	24	0
4	1 equiv	K_2CO_3	Acetone	56	48	0
5	1 equiv	TBD	Acetone	56	24	0

To facilitate this step, a Williamson ether synthesis was employed. Several reaction conditions were tested and are listed in Table 2. In the first experiment (entry 1), K_2CO_3 was used as a base in DMF at room temperature[44]. This approach was chosen because of its low reaction temperature, which minimizes the risk of undesired carbonate ring-opening and the S_N2-promoting character of (polar) DMF. However, no conversion was observed, potentially due to insufficient activation of the pronucleophilic alcohol group. To avoid this lack of reactivity, we turned to alternative conditions [44]. Higher temperatures were employed in the presence of tetrabutyl ammonium iodide (TBAI – a phase transfer agent) due to the poor solubility of the starting material [45]. This came with the known risk of decomposing the carbonate, however, again no conversion was observed. After reviewing the literature[46], then K_2CO_3 was used (entry 3) but with acetone as the solvent under reflux conditions. The aim was to promote the formation of the alkoxide, nevertheless, no conversion was observed even in the presence of TBAI (entry 4)[45]. Eventually (entry 5), TBD was used with TBAI[45] as it is known to be compatible with carbonates and is commonly used as a catalyst in ring-opening polymerization. Unfortunately, still no conversion was observed.

Since this Williamson ether synthesis did not provide the desired reactivity, a different approach was explored. A different linker molecule was necessary to couple the azobenzene to the carbonate. Due to the success with Steglich esterification, we designed a new bifunctional chain. This chain consists of one hydroxy and one carboxylic acid terminus, allowing to perform a two-step Steglich esterification. To obtain the C_6-linker, the corresponding precursor 6-hydroxy hexanoic acid would be needed. Unfortunately, the

latter is not commercially available as the hydroxy-acid obviously can undergo inter- and intra-molecular reactions affording (poly)esters and/or lactones. To synthesize the chain, we selected commercial ε-caprolactone, which was opened and sequentially protected with an isobutyl group[47]. This resulted in intermediate 4 in good yield and being purified by Kugelrohr distillation. To avoid side reactions during the coupling reaction with azobenzene, the latter was attached to the hydroxyl end of the chain by Steglich esterification[32,33]. Following this, the isobutyl protecting group was selectively cleaved using 4 N HCl. The newly formed azobenzene derivative was obtained with a 75% yield[48]. This selective cleavage regenerates the carboxylic acid in good yields. Finally, the unprotected carboxylic acid was used in a second Steglich esterification to yield **M2** in a good yield (60%, see Scheme 4).

5.3.1 Isomerization studies for Monomer 2 (**M2**)

UV-VIS: To determine the optimal irradiation time required to achieve a maximum conversion of *trans*-to-*cis* configured azobenzene, UV-VIS was employed. An initial spectrum was recorded without irradiation, followed by subsequent measurements taken every 20 seconds. As shown in Figure 13, the absorption band characteristic of the *trans*-isomer decreases with increasing irradiation time. Maximum photoisomerization was likely reached after 40 seconds, as after 60 seconds, no significant changes were observed[34].

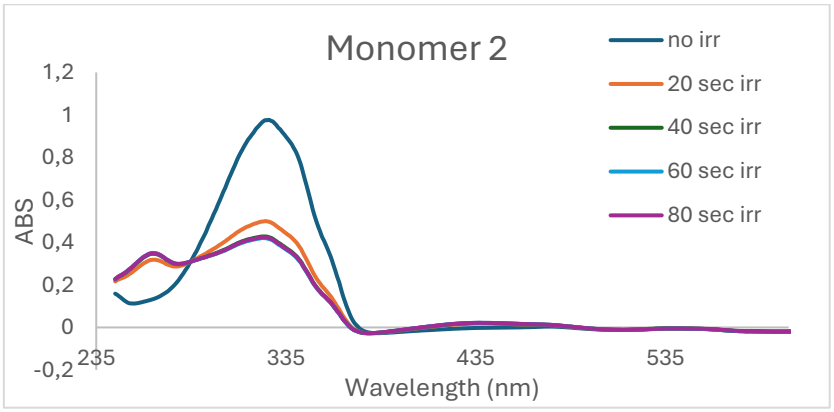

*Figure 13 UV-VIS of **M2**, and time of irradiation versus extent of photoisomerization from trans to cis.*

NMR: The same NMR studies (as for **M1**) were conducted for the second monomer (**M2**) with a special focus on the photo-responsive isomerization of the azobenzene unit. Figure 14 shows the corresponding ^{1}H-NMR spectra, before (black) and after (orange) UV irradiation for 100 seconds. Isomerization of the azobenzene from *trans* to *cis* is clearly visible, as the aromatic protons of the *trans*-isomer are decreasing in intensity, and new

peaks are observed for the *cis*-isomer. Before irradiation, the mixture of *trans* and *cis* is 92:8. After irradiation, the photostationary state was reached, and a ratio of 67:33 (*trans*-to-*cis*) was observed[34,36].

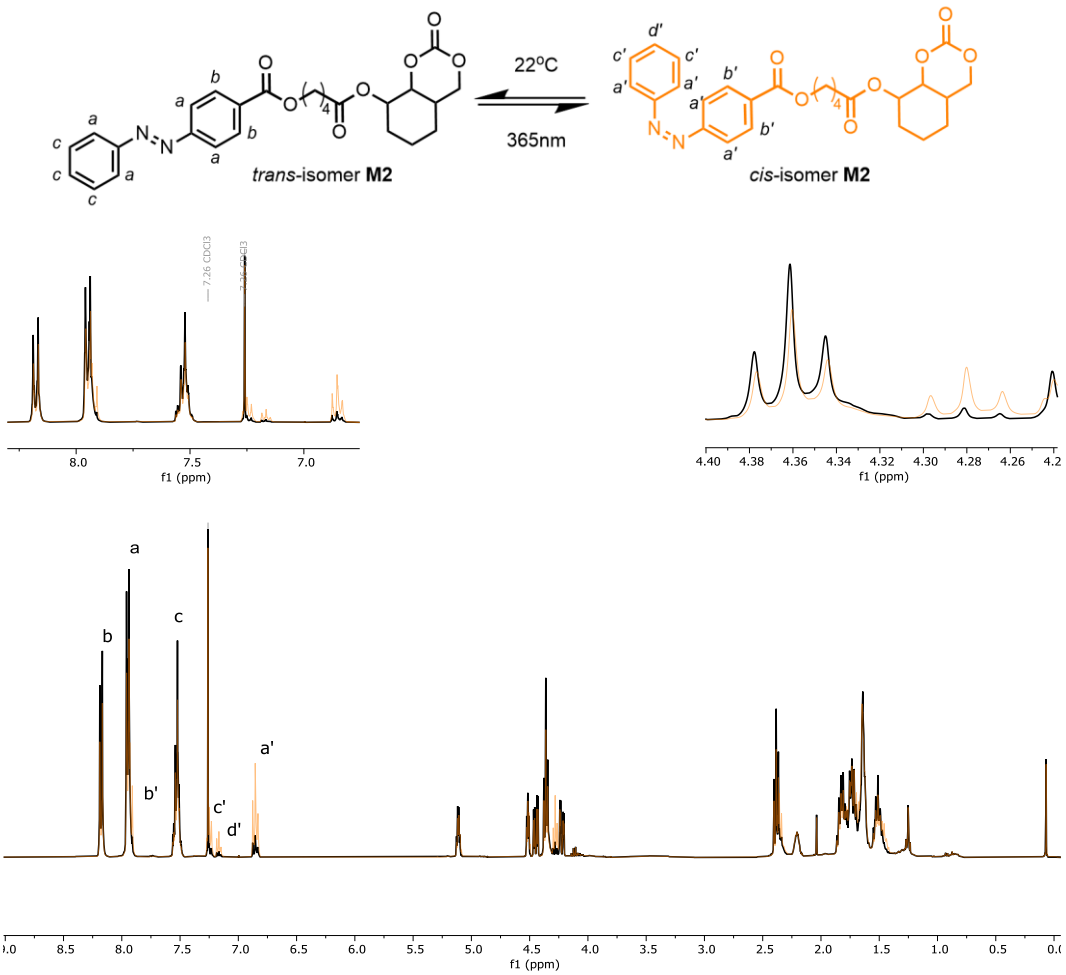

*Figure 14 ^{1}H-NMR spectrum of **M2**, the black trace is without irradiation, and the orange one is with irradiation with UV light at 365 nm.*

To evaluate the thermal (22-23°C) back-isomerization of the *cis*- to the *trans*-isomer of the photo-responsive unit, ^{1}H-NMR was employed. Figure 15 shows the spectrum, where the maximum back-isomerization ratio *trans-cis* (83:17) was observed after 48 hours. Before irradiation, the mixture of *trans* and *cis* is 92:8. After irradiation, the photostationary state was reached, with a *trans-cis* ratio of 67:33. As the monomer **M2** (just like **M1**) can undergo photoisomerization, it was also used for the ring-opening polymerization studies[37,38]. The half-life time of the back isomerization of the photo-responsive azobenzene from *cis* to *trans* was calculated. The half-life time of **M2** was $t_{1/2}$ = 0,693/0,0080 = 87 hours in normal conditions (stored in the fume hood, not in dark conditions) at 22-23 °C.

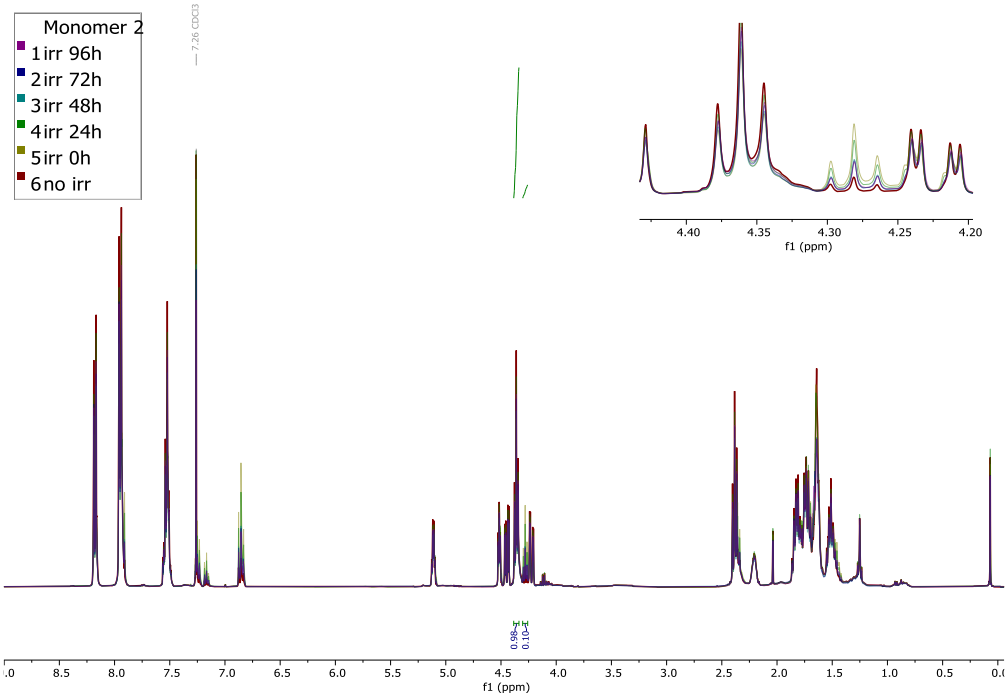

*Figure 15 **M2** relaxation after irradiation from cis back to trans.*

5.4 Ring-opening polymerization

As discussed in the introduction, there are various strategies for incorporating the photo-responsive azobenzene into polymers. A promising strategy is to directly incorporate the azobenzene into the backbone of the polymer[49,50]. This is expected to have the most pronounced effect and a bigger impact on the thermal and mechanical behavior. However, this method is synthetically challenging and requires advanced expertise. Thus, within this project, the photo-responsive azobenzene was first attached to the free alcohol group of the monomer, as the easy-functionalizable bicyclic carbonate precursor had been previously studied in the Kleij group[10]. Once the monomers **M1** and **M2** were successfully synthesized, they were subjected to ring-opening polymerization (ROP).

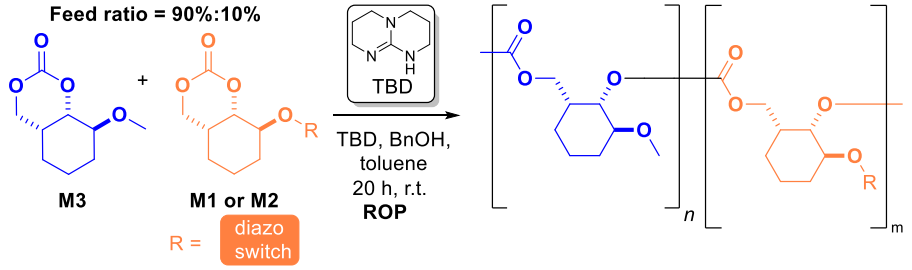

*Scheme 5 Ring-opening polymerization of **M1-3**.*

Two types of carbonate monomers were used in the polymerization, one functionalized with an azobenzene moiety (**M1** or **M2**) and the other one with a methoxy group (**M3**, Scheme 5). The methoxy-functionalized **M3** was present at a 90 mol% loading in the monomer feed and acts as a "dummy-monomer". This molecule was previously synthesized in the Kleij group[31]. The azobenzene-functionalized **M1** or **M2** were both used at a 10 mol% loading. Higher loadings of azobenzene-functionalized monomer will lead to enhanced steric hindrance in the polymer backbone[10]. This could limit the growth of the polymer chain, resulting in a lower molecular weight. However, high molecular weight is not ideal because higher M_n could mean higher T_g (until a certain level). If the T_g becomes too high, the solid-to-liquid transition is less likely to occur. Benzyl alcohol (BnOH) was used as an initiator, and TBD[20] served as an organocatalyst for the ROP. During the optimization, various parameters were adjusted, such as the loading of the initiator and catalyst, the temperature, and the reaction time. The monomer conversion was monitored by ^{1}H-NMR spectroscopy, while the number average molecular weight (M_n) and dispersity ($Đ$) of the purified polymer were determined by SEC (Size Exclusion Chromatography).

Polymer 1: The initial conditions for the ring-opening polymerization were based on a previously reported protocol by Kleij et al.[31]. Standard conditions for this type of ROP included both 2 mol% of initiator (benzyl alcohol) and catalyst (TBD), and a monomer concentration of 0.09 M in toluene at room temperature for 24 hours. In this initial optimization attempt, our main goal was to access a polymer of reasonable size (at least one photo-responsive azobenzene moiety) for the study of its properties. If needed, fine tuning of the reaction conditions would then improve conversion and dispersity. Under these conditions, the molecular weight was 1.60 kg/mol, the calculated degree of polymerization (DP) was 10 with a dispersity ($Đ$) of 1.4, indicating thus the formation of an oligomer. However, the molecular weight was not substantial, prompting further optimization. In the process related to entry 2, the reaction temperature was increased to 40 °C to accelerate polymer kinetics. This adjustment led to a 165% increase in M_n while the $Đ$ value remained the same, marking a significant improvement in polymer chain growth. In entry 3, both initiator and catalyst were reduced to limit the initiation sites. With less initiation, the ratio between propagation chains and monomers is higher, which may result in longer polymer chains. To our delight, this modification produced a 121% increase in the M_n with a slightly improved $Đ$ of 1.3 and DP of 13. In entry 4, the temperature was reduced to prevent side reactions, but no improvement in the M_n was observed. The process under

entry 5 involved changing the dummy monomer. The previously used methoxy-functionalized monomer (**M3**) was replaced with an ester-functionalized moiety. This was done to ensure that the methoxy substituent does not cause any hindrance in the polymerization. However, no significant improvement in the molecular weight was observed. This confirms that the methoxy-functionalized monomer does not affect the reaction. In the protocol of entry 6, the reaction was scaled up from 0.55 mmol to 1.32 mmol of total monomer while keeping the same concentration. This led to a slight increase in M_n to 3,51 kg/mol, a DP of 17 and a *Đ* value of 1.2. Considering all data, the process of entry 6 was the most promising overall.

*Table 3 Optimization table for the ring-opening polymerization of **M1**.*

Entry	[Diazo] (mol%)	[MeO] (mol%)	TBD/BnOH (mol%)	Solv. (M)	C. (%)	T (ºC)	t (h)	*Đ*	M_n (kg/mol)	*DP*
1	10	90	2 + 2	TOL (0.09)	88	r.t.	24	1.4	1.60	10
2	10	90	2 + 2	TOL (0.09)	88	40	24	1.4	2.65	13
3	10	90	1 + 1	TOL (0.09)	85	40	24	1.3	3.21	16
4	10	90	1 + 1	TOL (0.09)	88	r.t.	24	1.2	2.71	13
5[a]	10	90	1 + 1	TOL (0.09)	85	40	24	1.7	2.23	10
6[b]	10	90	1 + 1	TOL (0.09)	90	40	24	1.2	3.51	17

[a]Ester-based monomer used. [b] Three-fold scaled-up experiment.

The polymer **P1** has a *Đ* range of 1.2-1.7, which falls in the range found in the literature[31] for polycarbonates with bulky substituents (1.2 to 2.2). The molecular weight observed between 1.6-3.5 kg/mol aligns with the expected range for such systems, which varies from 2.0 to 9.7 kg/mol. The total monomer conversion of this polymerization is very constant and reaches up to 90%. The initiation of the polymerization, therefore is likely not the problem to reach high(er) molecular weight. The relatively low molecular weight can be ascribed to the bulky nature of the azobenzene-derived monomer **M1**, whose incorporation may significantly slow down further propagation. Simultaneous chain-transfer events induced by protic impurities (alcohols, H_2O) would then become more relevant and competitive, thereby causing a lower than expected molecular weight for the envisioned polymer[31, 51].

In Figure 16, the solid polymer **P1** is shown in its initial, non-irradiated state as a light orange material (*trans*). After irradiation, the polymer appears as a darker orange solid material (*cis*-enriched), indicating isomerization after irradiation, as also confirmed by ^{1}H-NMR (see SI Figure 41). The color change serves as a visual indicator of the isomerization process. The polymer was also successfully processed into a film using a hot press. The solid polymer was placed in a 10 mm-by-10 mm mold and pressed at 90 °C under 1 ton of pressure for 5 times during 2.5 minutes to prevent air bubbles. This procedure resulted in the film shown in Figure 16. The film was irradiated by UV light (365 nm), and ^{1}H-NMR confirmed the *trans*-*cis* isomerization (see SI figure 40). These results demonstrate the polymers' photo-responsive behavior in the solid state and when prepared as a film.

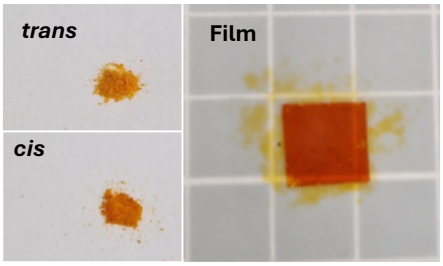

*Figure 16 Irradiation of solid **P1** and a film of **P1**.*

DSC and TGA were also measured for **P1**. The thermogravimetric analysis measures the mass change of a sample as a function of temperature or time. This evaluates the thermal stability of the polymer. A TGA analysis for **P1** was measured, and at 170 °C (T_d^5), significant weight loss started to occur. This loss in weight indicates that after 170 °C, part of the polymer degrades. DSC was measured before and after photoisomerization of the azobenzene. No difference in T_g is observed after the isomerization of the azobenzene. The T_g of both polymers was 59 °C, which indicates that the presence of an azobenzene in the polymer backbone does not have a significant effect on the T_g. However, isomerization is definitely observed and proved by various techniques, as shown in Chapter 5.5. A clear color change is observed, which is also in line with the isomerization of the azobenzene. Although the presence of azobenzene units is clear, the relative amount that is incorporated may need to be increased to be able to observe changes in the thermal and mechanical behavior, whereas higher molecular weight polymers could also induce more significant changes. An alternative design could be to separate the azobenzene units better from the backbone of the polymer, and this approach was therefore explored.

Polymer 2: Monomer **M2** was successfully synthesized using similar reaction conditions as before in the synthesis of **M1**, and it was then used in ring-opening polymerization. A small optimization was first performed, starting with the best conditions determined for the polymerization of **M1**. A slight improvement was observed when the temperature was

increased to 60 °C. The conversion was calculated from the crude ^{1}H-NMR, and the M_n was determined by SEC. **P2** is likely even more bulky (voluminous) than **P1**, due to the presence of an additional alkyl chain between the carbonate and the azobenzene. The molecular weight of **P2** did not exceed 2.29 kg/mol. The *Đ* of this anionic ROP was in both experiments (entries 1 and 2) 1.4 and the calculated DP´s were 9 and 11 (Table 4). These data concur with those in the literature[31,51] for similar ROP processes involving monomers with bulky substituents.

*Table 4 ROP experiments carried out for **P2**.*

Entry	[Diazo] (mol%)	[MeO] (mol%)	TBD/BnOH (mol%)	Solv. (M)	C. (%)	T (º C)	t (h)	*Đ*	M_n (kg/mol)	*DP*
1	10	90	1 + 1	TOL (0.09)	88	40	24	1.4	2.00	9
2	10	90	1 + 1	TOL (0.09)	89	60	24	1.4	2.29	11

DSC and TGA analyses were done for **P2**, and a T_d^5 was observed at 220 °C. This loss in weight indicates that beyond 220°C, part of the polymer is starting to degrade. DSC was measured before and after photoisomerization of the azobenzene. The T_g in both cases was 32 °C, which indicates that the presence of the azobenzene unit in **P2** does not have a significant effect on the T_g.

5.5 Isomerization studies for polymers **P1** and **P2**

NMR: After confirming that both monomers undergo isomerization upon irradiation with UV light (365 nm) and can be successfully polymerized by ROP, the photo-isomerization of the polymer products was further investigated. ^{1}H-NMR was employed to monitor the *trans*-to-*cis* isomerization. In both cases, a decrease in the intensity of the aromatic protons of the *trans*-isomer was observed, as illustrated in Figures 17 and 18, along with the appearance of new peaks for the *cis*-isomer. These spectral changes confirm a successful isomerization from *trans*-to-*cis* for both polymers **P1** and **P2**. Before irradiation, **P1** was a mixture of 83:17 *trans*/*cis* and **P2** was an 86:14 *trans*/*cis* mixture. After irradiation, the photostationary state was reached, and a *trans*:*cis* ratio of 46:54 (for **P1**) and 46:54 (for **P2**) was observed. Interestingly, we observe a better photostationary state for **P1** and **P2** than in the case of **M1** and **M2**[34,36].

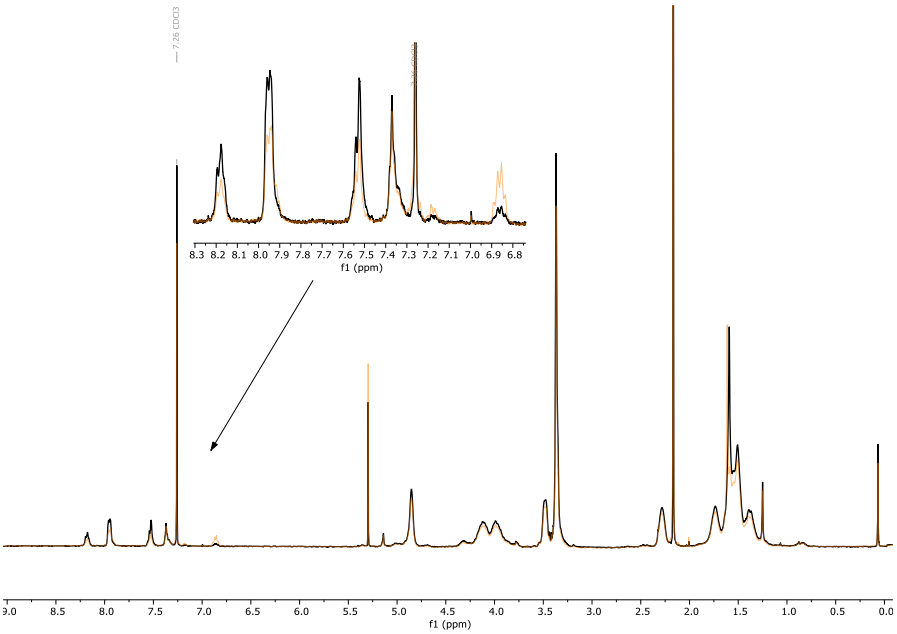

*Figure 17 ^{1}H-NMR spectrum of **P1**, where the black trace is the non-irradiated sample and orange one the irradiated sample using UV light (365 nm).*

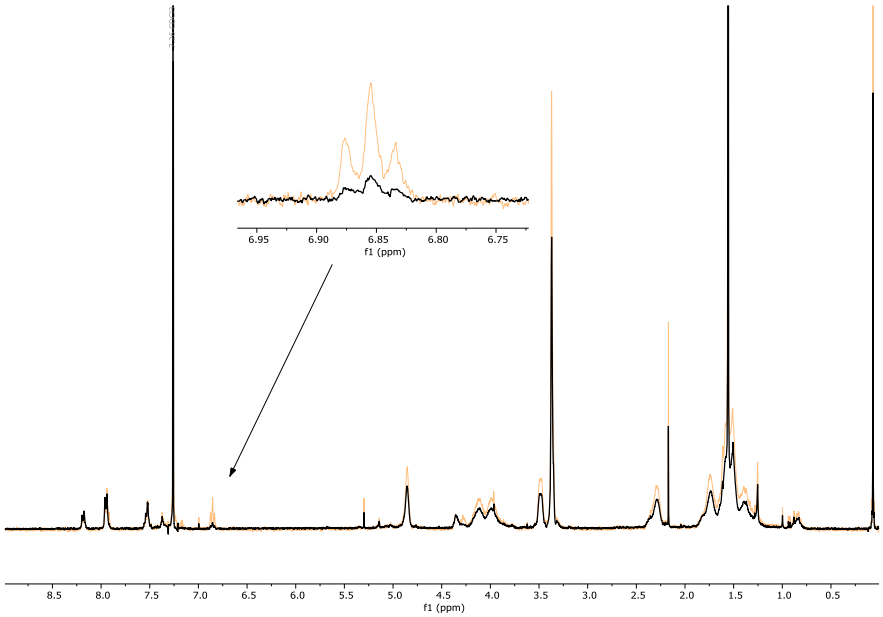

*Figure 18 ^{1}H-NMR spectrum of **P2**, where black is the non-irradiated sample and the orange one the irradiated using UV light (365 nm).*

When exploring the thermal (22-23ºC) relaxation of the *cis*-to-*trans* back-isomerization, ^{1}H-NMR was employed (Figures 19 and 20). The sample was measured before irradiation, immediately after UV irradiation (t = 0 hours), and subsequently over a period of several days. For both **P1** and **P2**, a maximum conversion level is observed after 72 hours, showing

for **P1** a 76:24 *trans*/*cis* ratio and for **P2** a 79:21 *trans*/*cis* ratio. These data represent the equilibrium for both polymers after photoirradiation followed by relaxation [37,38]. The half-life time of the back isomerization of the photo-responsive azobenzene from *cis* to *trans* was calculated. The half-life time of **P1** was $t_{1/2}$ = 0,693/0,0076 = 91 hours and for **P2** $t_{1/2}$ = 0,693/0,0070 = 99 hours in normal conditions (stored in the fume hood, not in dark conditions) at 22-23 °C. If we compare **M1** and **M2** with **P1** and **P2**, we observe very comparable results.

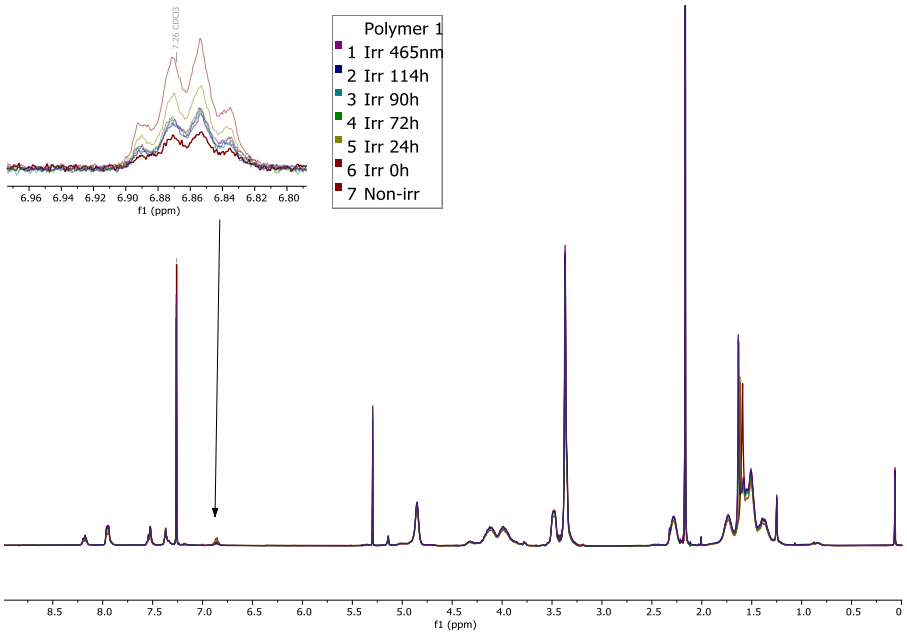

Figure 19 ***P1*** *relaxation to a thermodynamic equilibrium mixture after irradiation.*

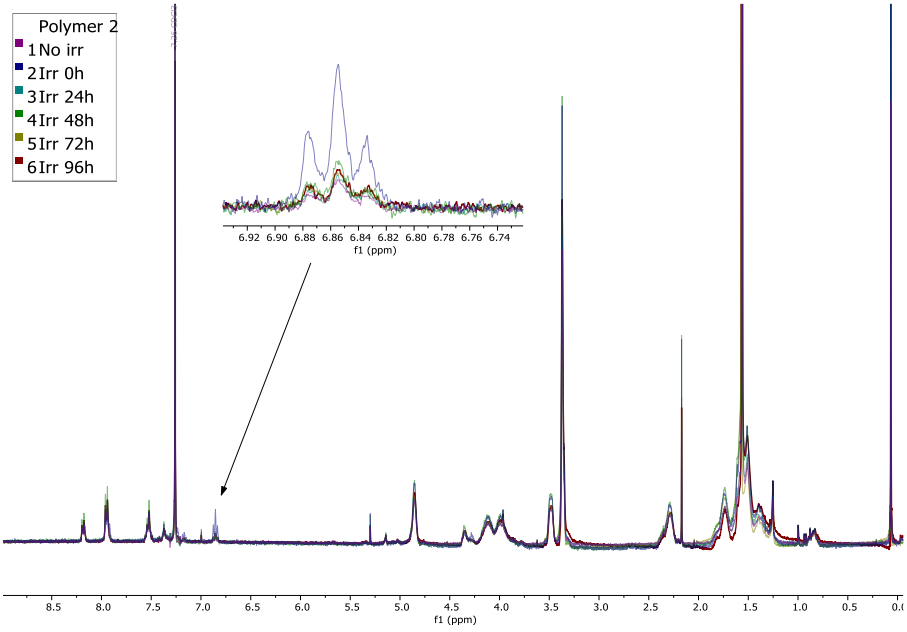

Figure 20 ***P2*** *relaxation to a thermodynamic equilibrium mixture after irradiation.*

UV-VIS: To determine the required irradiation time for maximum photo-isomerization, UV-VIS spectra were measured at different time intervals. As shown in Figure 21, **P1** reaches its maximum conversion after 20 seconds of irradiation. When irradiated for an additional 20 seconds, no significant difference was observed. In contrast, **P2** required a total of 40 seconds to reach its maximum isomerization. The required irradiation time for maximum photo-isomerization is comparable with the monomers **M1** and **M2**[34].

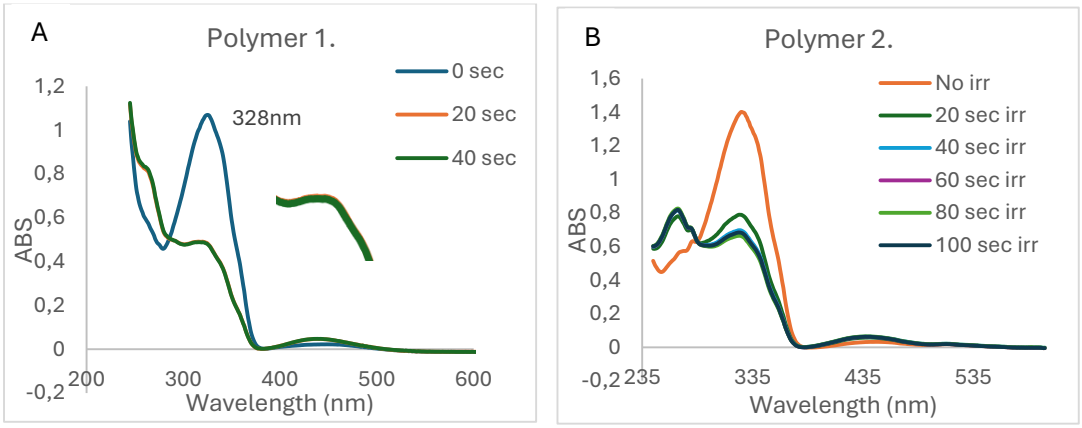

*Figure 21 A: **P1**, B: **P2**, UV-VIS spectrum of duration of irradiation to achieve maximum isomerization from trans to cis.*

UV-VIS: To investigate the thermal (22-23 °C) back isomerization of **P1** from *cis* to the *trans* configuration, UV-VIS was employed. An initial spectrum was measured before irradiation, followed by irradiation with UV light. The cuvette was placed in a dark spectrometer chamber to prevent further photo-isomerization. A spectrum was measured every 15 minutes to monitor the thermal relaxation process. As shown in Figure 22, a significant difference in absorption was observed. The maximum absorption peak corresponding to the *trans*-isomer at 325 nm decreased from 1.27 (*trans*) to 0.82 (*cis*), thus indicating a successful isomerization process. Additionally, a new peak appeared at 445 nm, which corresponds to the *cis*-isomer. After 510 minutes of relaxation, full conversion back to the original *trans*-isomer was observed. Furthermore, the spectral data can be used to extract the kinetic parameters of the thermal isomerization process.

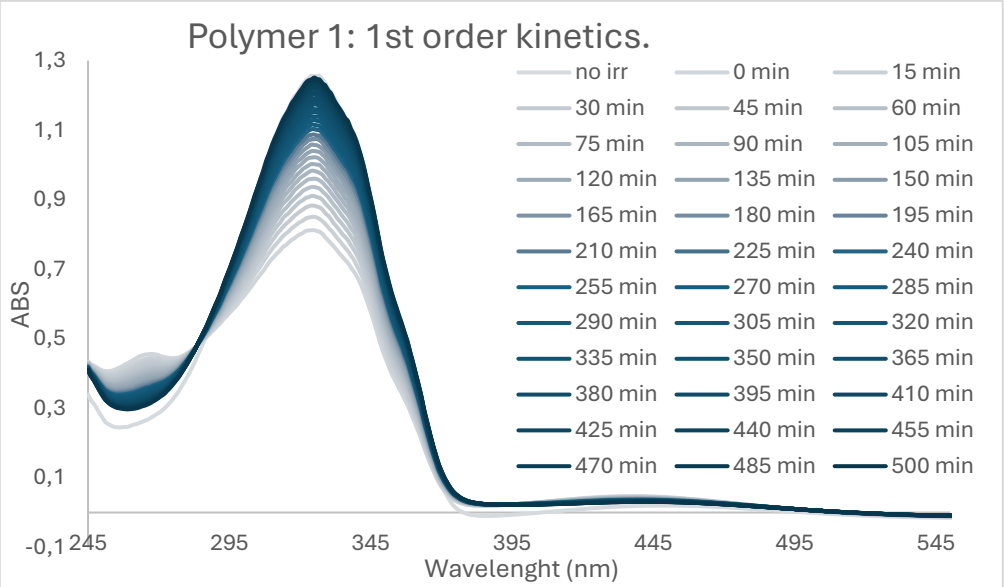

*Figure 22 Kinetic study using UV-VIS referring to the back-isomerization of **P1**.*

Kinetics: The photoisomerization of the azobenzene and the kinetic data were analyzed to determine the order of the reaction (Figure 23)[52]. The absorbance of the *trans* isomer was plotted against time (in min). Also, the natural logarithm of the proportion of $A_{cis}^{325\ nm}$ of the *cis* isomer ($A_{cis}^{325\ nm} = A_{obs}^{325\ nm} - A_{cis_{max}}^{325\ nm}$) was plotted against the time (in min). A first-order kinetic plot is observed in relation to the azobenzene fragment, indicating that the isomerization occurs via a unimolecular isomerization process. This aligns with the literature reports for azobenzene-related compounds[48]. With this data, the half-life time of the back isomerization could be calculated. This is the time required for the photoisomerization process to decrease to half of its initial value. Calculated using the first-order relation $t_{1/2} = 0{,}693/k$ (in this case, k is the rate constant from the slope), the half-life time of this process is $t_{1/2} = 0{,}693/0{,}0055 = 126$ minutes (in dark conditions)[37].

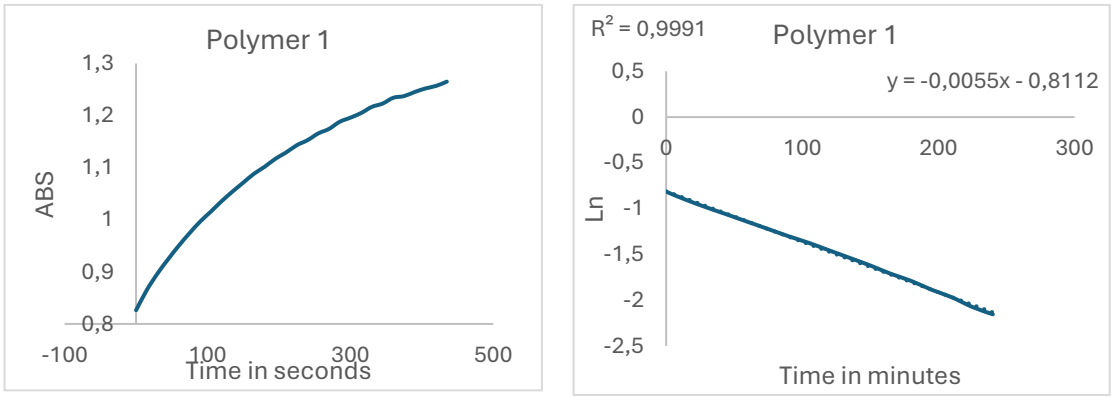

*Figure 23 Kinetic data using UV-VIS referring to the back-isomerization of **P1** to determine the order of the reaction.*

UV-VIS: for **P2**, the same study was done. First, the non-irradiated sample was measured by UV-Vis (Figure 24). The sample was irradiated with UV light and measured again. A large decrease in intensity was observed at 325 nm, and an increase was observed at 435 nm. This indicates the isomerization from *trans* to *cis*. After 750 minutes, the *cis* isomer is fully converted back to *trans* by relaxation.

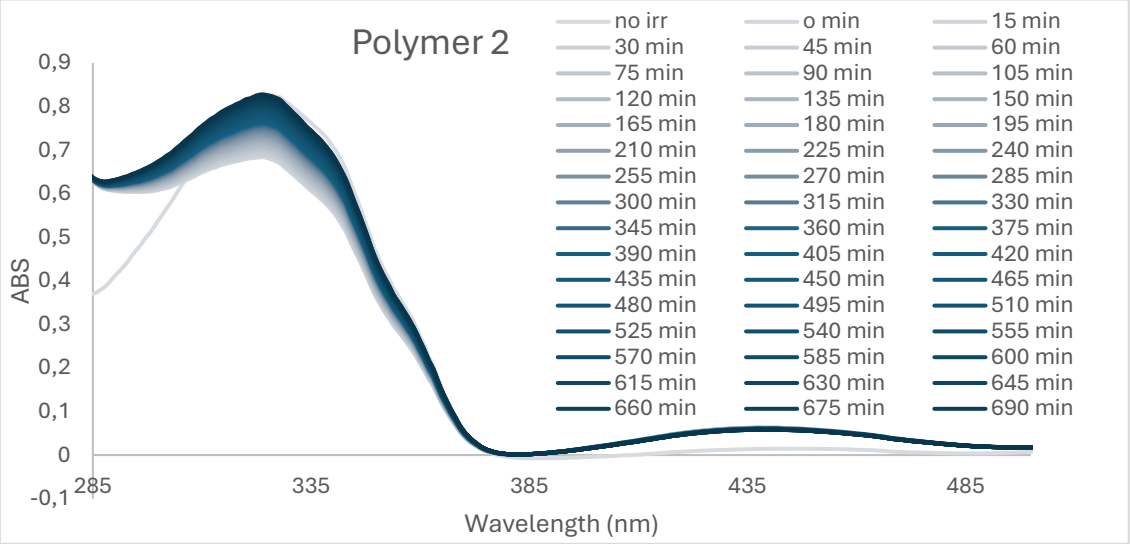

*Figure 24 Kinetic study using UV-VIS referring to the back-isomerization of **P2**.*

Kinetics: In Figure 24, the kinetics of the back isomerization of **P2** was analyzed[52]. Following the same method used for **P1**, the absorbance of the trans isomer was plotted against time (in min). The exponential decay pattern suggests a 1st order kinetics. To confirm this, the ln of proportion the *cis* isomer ($A_{cis}^{325\ nm} = A_{obs}^{325\ nm} - A_{cis_{max}}^{325\ nm}$) against time was plotted, resulting in a linear curve with an R^2 of 0,9907. The half-life time was calculated: $t_{1/2}$ = 0,693/0,003 = 231 minutes[37]. This indicates that after 231 minutes (in dark conditions), half of the *cis* has isomerized back to *trans*.

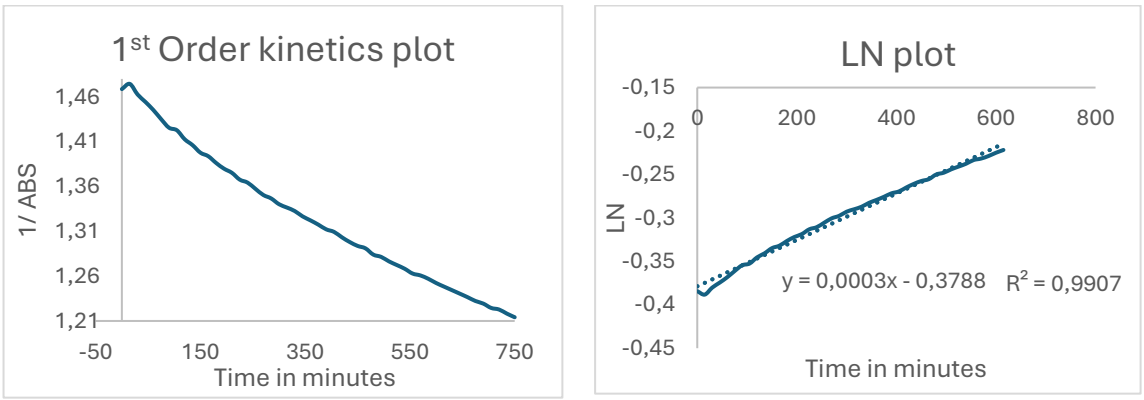

*Figure 25 Kinetic data using UV-VIS referring to the back-isomerization of **P2** to determine the order of the reaction.*

6. Summary & Conclusions

In conclusion, two monomers **M1** and **M2** based on a bicyclic carbonate scaffold were successfully synthesized. The cyclic carbonate precursor was functionalized with a photo-responsive azobenzene unit, leading to the successful synthesis of **M1** and **M2**. **M1** was successfully synthesized by Steglich esterification in good yields of up to 76%. Its photo-responsive behavior was confirmed through successful *trans* to *cis* isomerization upon irradiation with UV light (365 nm). Monomer **M2** incorporates a spacer between the cyclic carbonate and the azobenzene unit. This multistep synthesis also produced the final product in an appreciable yield (60%) and demonstrated similar *trans* to *cis* isomerization under UV light. All intermediates and products of these two routes were characterized by ^{1}H-NMR, ^{13}C-NMR, FTIR, MS and UV-Vis.

Following successful photo-isomerization, both monomers **M1** and **M2** were polymerized. This was done by anionic ring-opening polymerization, using benzyl alcohol and TBD, as initiator and catalyst, respectively. **P1** was obtained, after optimization, with a number average molecular weight of 3.51 kg/mol and a $Đ$ of 1.2. **P2** was obtained with a molecular weight of 2.29 kg/mol and a $Đ$ of 1.4. Both polymers were irradiated, and approximately 50% of the photo-responsive azobenzene moieties were isomerized using UV light (365 nm). After irradiation, successful back-isomerization from *cis* to *trans* was observed. Kinetic studies confirmed a 1st order dependence for the back-isomerization process involving the azobenzene fragment. Unfortunately, no T_g change could be observed after irradiation.

Therefore, in order to induce significant changes upon photoirradiation, modifications to the polymer are needed to create a solid-to-liquid transition. One possible design involves incorporating the azobenzene moiety directly in the polymer backbone, though this requires a careful design of the synthetic process. Nevertheless, the synthesized photo-responsive polycarbonates **P1** and **P2** provide insight into the design of stimuli-responsive materials and a solid reference for future azobenzene-derived macromolecules in the field.

7. Outlook

This thesis has provided a broad perspective on the possibilities of photo-responsive azobenzene units embedded in polycarbonate-based polymers. With the acquired knowledge and expertise, in future work, the research group is well-prepared to continue working on azobenzene-derived polycarbonates and related macromolecules.

One promising direction (as already mentioned in section 7) is to incorporate the photo-responsive azobenzene moiety directly into the backbone of the polycarbonate (Figure 26) This modification could potentially have a more significant influence on the thermal and mechanical behavior. There are several possible approaches to achieve this: (***1***) connecting two linear oligomers attached to a bifunctional photo-responsive azobenzene, shown in Figure 26A. (***2***) A second approach is to directly embed an azobenzene into the backbone of the polymer illustrated in Figure 26B. However, these approaches are synthetically more demanding and are thus recommended for future work.

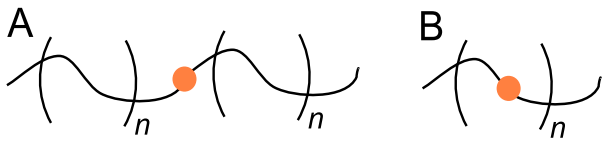

Figure 26 Different ways of embedding photo-responsive azobenzene moieties in macromolecules.

8. Experimental section

8.1 General remarks

If needed, solvents were dried using an Innovative Technology PURE SOLV solvent purification system. Reactions were monitored by TLC and ^{1}H NMR ($CDCl_3$). TLC was carried out on 0.25 mm aluminum-backed sheets coated with 60 F254 silica gel (Merck). Visualization of the silica plates was achieved using a UV lamp (λ = 254 nm) and/or by heating plates that were dipped in a ceric ammonium molybdate solution. Flash chromatography was carried out with commercially purchased silica gel 60 (70-230 mesh, from Sigma/Aldrich) using the indicated eluent system. Benzyl alcohol was dried over calcium hydride and distilled under reduced pressure before its use. TBD was dissolved in CH_2Cl_2, stirred over calcium hydride, filtered and dried in vacuum prior to use. The Irradiation studies were done by using a Hönle UV technology LED cube100IC, UV-oven, on 365nm with 70% intensity.

NMR Spectroscopy: NMR spectra were obtained on a Bruker 400 MHz, a 500 MHz or a 500 MHz with cryoprobe spectrometers equipped with probe-heads capable of producing gradients in the z direction with a maximum strength of 53.5 G/cm. ^{1}H, ^{13}C and NMR chemical shifts are reported in parts per million (ppm), relative to tetramethylsilane (TMS) for ^{1}H and ^{13}C NMR experiments with the residual solvent peak used as an internal reference. Multiplicities are reported as follows: singlet (s), broad band (br), d (doublet), dd (doublet of doublets), triplet (t) and multiplet (m).

Mass Analysis: High Resolution Mass Spectrometry (HRMS) data was recorded using two different methods depending on the complex to be analyzed. ESI-MS analyses were performed in a MicroTOF Focus mass spectrometer (Bruker Daltonics) by direct injection. All MS data were collected by the Research Support Unit at ICIQ.

Thermal Analysis: Differential scanning calorimetry (DSC) analyses for glass transition temperatures (T_g) determination were measured under an N_2 atmosphere using Mettler Toledo equipment (model DSC822e). Samples were weighed into 40 µL aluminum crucibles and subjected to three heating cycles at a heating rate of 10 °C/min. Thermogravimetric analyses (TGA) were recorded under an N_2 atmosphere using Mettler Toledo equipment (model TGA/SDTA851). Samples were weighed into 40 µL aluminum crucibles and heated

to 600 ºC at a heating rate of 10 °C/min. All thermal data were collected by the Research Support Unit at ICIQ.

Size Exclusion Chromatography (SEC) measurements were performed using an Agilent 1200 series HPLC system, equipped with PSS SDV Analytical linear M SEC column (8 x 300 mm; 5 µm particle size) in tetrahydrofuran at 30 °C at a flow rate of 1 mL·min^{-1}. Samples were analyzed at a concentration of around 1 mg·mL^{-1} after filtration through a 0.45 µm pore-size membrane. M_n, M_w, and $Đ$ data were derived from the RI signal by a calibration curve based on polystyrene standards (polystyrene standards obtained from Polymer Standards Service) for the analysis of the polymers. The SEC samples were prepared by dissolving the polymer (3–5 mg) in THF (2 mL) and filtering the solution through a 0.45 µm pore-size membrane.

Synthetic preparations: Al-centered aminotriphenolate complex (**C1)** was synthesized according to previously reported procedures[16]. All the monomers were dissolved in dichloromethane (1 to 5 mL) and the solutions stirred for 16 h in the presence of anhydrous CaH_2. The solid part was then removed through filtration, the residue was evaporated under vacuum yielding the corresponding dried monomer, which was then used without further purification.

8.2 Procedure for the preparation of monomer backbone

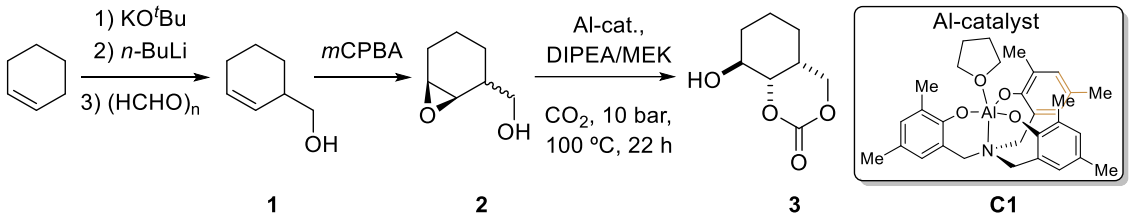

1 **2** **3** **C1**

Step 1: A 500 mL round bottom flash was charged with cyclohexene (54 mL, 0.53 mol), KO^{t}Bu (6.8 g, 60.4 mmol), and the resulting suspension was degassed for 30 min with Argon. The mixture was cooled to 0 °C, and *n*BuLi (1.6 M in Hexanes, 40 mL, 64 mmol) was added dropwise. The resultant mixture was stirred at the same temperature for 2 h, then allowed to warm to room temperature and stirred for another 16 h. The resultant pale-yellow suspension was cooled to 0 °C and (HCHO)$_n$ (2 g, 66.4 mmol) was added. The reaction mixture was allowed to warm to room temperature and heated to 60 ºC for 3 h. Subsequently, the mixture was cooled to 0 °C and quenched with a saturated aqueous

$NaHCO_3$ solution (40 mL). The mixture was extracted with CH_2Cl_2 (3 × 40 mL). The combined organic phases were washed sequentially with a saturated aqueous $NaHCO_3$ solution (40 mL) and brine (40 mL), dried over $MgSO_4$, and concentrated *in vacuo* to give the desired product **1** in 49% yield as colorless oil.

Step 2: To a solution of **1** (2.5 g, 22.3 mmol, 1 equiv.) in dry MeOH (112 mL, 0.2 M) at 0 °C, *m*CPBA (7.5 g, 33.5 mmol, 1.5 equiv., 77% pure) was added portion-wise. The reaction mixture was allowed to warm to room temperature and then stirred for 16 h. The solvent was removed, the residue was dissolved in CH_2Cl_2 and then washed with Na_2CO_3. The organic phase was dried over $MgSO_4$, concentrated, and purified through column chromatography (hexanes: ethyl acetate, 6:4 v/v) to obtain the epoxy alcohol (**2**) in 45% as a colorless oil being an 8:2 mixture of *syn* and *anti*-isomers.

Step 3: A 25 mL stainless-steel reactor was charged with **2** (1.2 g, 9.3 mmol, 1 equiv), MEK (5.0 mL, 1.9 M), **C1** (100 mg, 0.19 mmol, 2 mol%), and DIPEA (175 µL, 0.94 mmol, 10 mol%). The reactor was purged three times and then charged with CO_2 (10 bar). The mixture was stirred at 100 °C for 22 h, then cooled with an ice/water bath and carefully depressurized. The solvent was removed *in vacuo* and the resulting product was purified by flash chromatography (hexanes: ethyl acetate 1:1), affording the desired product **3** in 42% yield as a pale-yellow solid[10].

Cyclohex-2-en-1-ylmethanol (1). Yellow oil, 49% yield. **^{1}H-NMR** (400 MHz, $CDCl_3$) δ 5.87 – 5.78 (m, 1H), 5.62 – 5.55 (m, 1H), 3.54 (d, J = 6.1 Hz, 2H), 2.37 – 2.25 (m, 1H), 2.05 – 1.93 (m, 2H), 1.85 – 1.68 (m, 2H), 1.46 – 1.32 (m, 2H). The spectral data correspond to the literature[10].

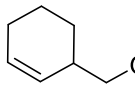

(7-oxabicyclo[4.1.0]heptan-2-yl)methanol (2). Yellow oil, 1:4 mixture of *syn/anti* isomer, 45% yield. **^{1}H-NMR** (500 MHz, $CDCl_3$) δ 3.73 (dd, *J* = 10.7, 5.7 Hz, 1H), 3.64 (dd, *J* = 10.7, 7.0 Hz, 1H), 3.18 (m, 1H), 3.09 (m, 4.0, 1.0 Hz, 1H), 2.13 – 2.00 (m, 2H), 1.69 (m, 2H), 1.60 – 1.53 (m, 1H), 1.43 – 1.35 (m, 2H), 0.95 (m, 1H); The spectral data correspond to the literature[10].

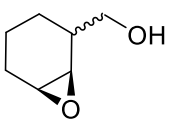

8-hydroxyhexahydro-4*H*-benzo[*d*][1,3]dioxin-2-one (3). Yellow oil, 42% yield. **^{1}H-NMR**

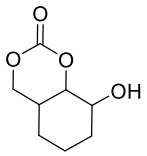

(500 MHz, $CDCl_3$) δ 4.48 – 4.40 (m, 2H), 4.25 (dd, *J* = 11.0, 3.9 Hz, 1H), 4.11 – 4.05 (m, 1H), 2.40 – 2.32 (m, 1H), 1.89 – 1.79 (m, 1H), 1.79 – 1.64 (m, 1H), 1.67 – 1.61 (m, 1H), 1.63 – 1.53 (m, 4H). The spectral data correspond to the literature[10].

8.3 Synthesis of Monomer 1

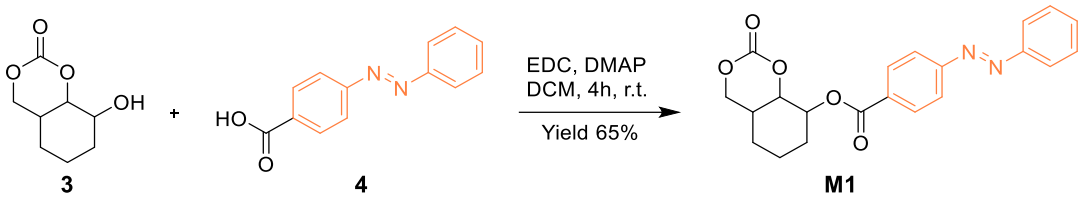

3 **4** **M1**

To a solution of carbonate (**3**) (1 equiv) and DMAP (1.1 equiv) in dry CH_2Cl_2 (0.2 M), carboxylic acid (**4**) was added (1.1 equiv) followed by addition of EDC (1 equiv). The resulting mixture was stirred at room temperature for 4 h. The resulting organic phase was washed three times with aq. 2 M HCL, three times with $NaHCO_3$, one time with brine and dried over $MgSO_4$, filtered and concentrated under vacuum, to give the desired products in 78% yield[31].

(*E/Z*)-8-(4-(phenyldiazenyl)benzoyl)hexahydro-4*H*-benzo[*d*][1,3]dioxin-2-one (M1).

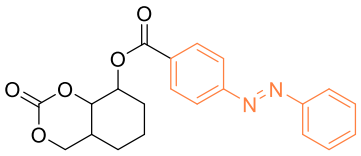

Orange solid, *E/Z* >90:10, 76% yield. **^{1}H-NMR** (400 MHz, $CDCl_3$) δ 8.24 – 8.14 (m, 2H), 8.04 – 7.93 (m, 4H), 7.60 – 7.49 (m, 3H), 5.40 (q, *J* = 3.6 Hz, 1H), 4.75 (t, *J* = 3.6 Hz, 1H), 4.53 (dd, *J* = 11.1, 3.7 Hz, 1H), 4.29 (dd, *J* = 11.1, 2.4 Hz, 1H), 2.41 – 2.30 (m, 1H), 2.04 – 1.90 (m, 2H), 1.89 – 1.65 (m, 4H). **^{13}C-NMR** (101 MHz, $CDCl_3$) δ 164.6, 155.4, 152.5, 147.6, 132.0, 131.2, 130.8, 129.3, 123.3, 122.9, 76.0, 72.2, 69.4, 28.8, 24.8, 22.5, 18.9. **IR (neat, CM^{-1}) v:** 2925-2866 (W), 1757 (S), 1709 (S). **ESI (+)** Calculated for $[C_{21}H_{21}N_2O_5]^+$ ($[M+H]^+$) 381.1452. Found 381.1445.

8.4 Synthesis of Monomer 2

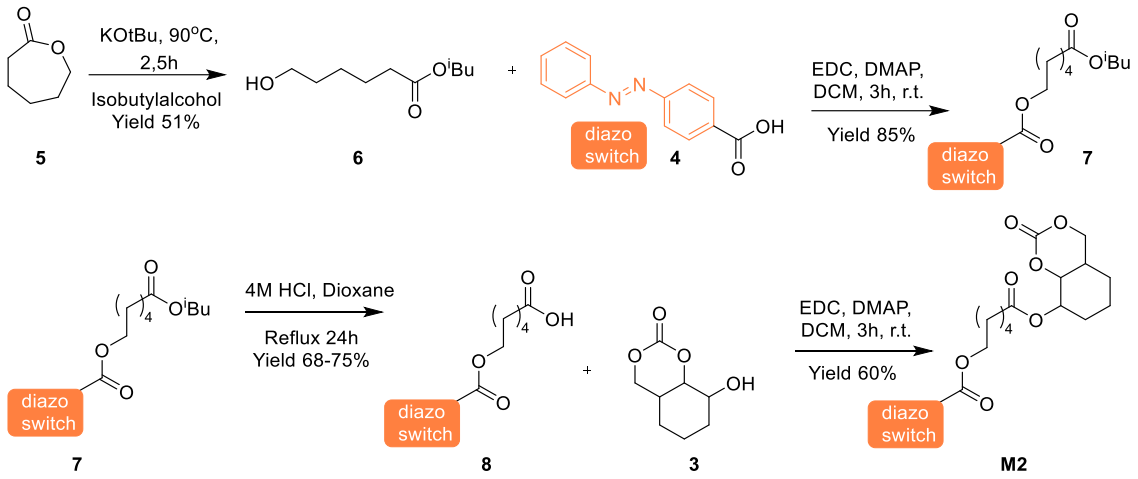

Step 1: ε-Caprolactone (**5**) (3.00 g, 26.3 mmol) and 3.24 g (28.4 mmol) of potassium *tert*-butoxide were refluxed for 2.5 h in 100 mL of *iso*-butyl alcohol. After diluting with diethyl ether, the reaction mixture was washed with water and brine, dried over magnesium sulfate, and concentrated on a rotary evaporator. Distillation (148°C, 29 mbar) afforded 2.54 g (51%) of *iso*-butyl 6-hydroxyhexanoate (**6**).

Step 2: To a solution of alcohol (**6**) (1 equiv) and DMAP (1.1 equiv) in dry CH_2Cl_2 (0.2 M), carboxylic acid (**4**) was added (1.1 equiv) followed by addition of EDC (1 equiv.). The resulting mixture was stirred at room temperature for 4 hours. The resulting organic phase was washed three times with 2M HCl, three times with $NaHCO_3$, one time with brine, and dried over $MgSO_4$, filtered, and concentrated under vacuum, to give the desired product (**7**).

Step 3: A solution of azobenzene *iso*-butyl ester (**7**) (175 mg, 0.44 mmol, 1 equiv.) in 1,4-dioxane (7 mL) was treated with 4 N HCl (10 mL) and refluxed for 1.5 hours. Upon cooling to 20 °C, a white precipitate formed. The 1,4-dioxane was removed on the rotary evaporator; the solid was collected by vacuum filtration, washed with water, and dried to constant weight to give 109 mg (68%) of compound **8**.

Step 4: To a solution of carbonate (**3**) (1 equiv.) and DMAP (1.1 equiv.) in dry CH_2Cl_2 (0.2 M), carboxylic acid (**8**) was added (1.1 equiv.) followed by addition of EDC (1 equiv.). The resulting mixture was stirred at room temperature for 4 hours. The resulting organic phase was washed three times with aq. 2M HCl, three times with $NaHCO_3$, one time with brine,

and dried over $MgSO_4$, filtered, and concentrated under vacuum. The crude was flushed over silica (solvent) to give the desired products (**M2**)[31,47,53].

Isobutyl 6-hydroxyhexanoate (6). Colorless liquid, 51% yield. **^{1}H-NMR** (400 MHz, $CDCl_3$) δ

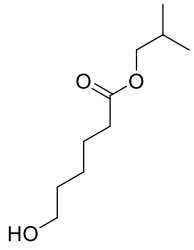

3.81 (d, *J* = 6.6 Hz, 2H), 3.59 (t, *J* = 6.6 Hz, 2H), 2.29 (t, *J* = 7.5 Hz, 2H), 2.02 (s, 1H), 1.88 (dt, *J* = 13.4, 6.7 Hz, 1H), 1.68 – 1.49 (m, 4H), 1.42 – 1.30 (m, 2H), 0.89 (d, *J* = 6.7 Hz, 6H). **^{13}C-NMR** (101 MHz, $CDCl_3$) δ 173.9, 70.4, 62.5, 34.2, 32.3, 27.7, 25.3, 24.7, 19.1. **IR (neat, CM^{-1}) v:** 3400 (W), 2936-2873 (W), 1733 (S), **ESI (+)** Calculated for $[C_{10}H_2O_3]^+$ ([M+Na]$^+$) 211.1305. Found 211.1312.

6-isobutoxy-6-oxohexyl (*E/Z*)-4-(phenyldiazenyl)benzoate (7). Orange liquid, *E/Z* >90,

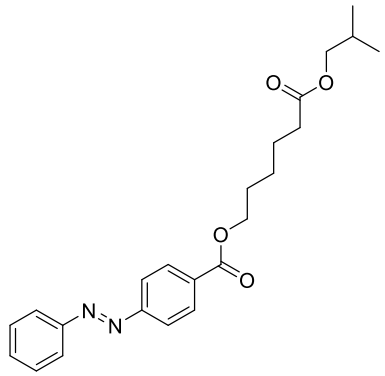

86% yield. **^{1}H-NMR** (400 MHz, $CDCl_3$) δ 8.21 – 8.16 (m, 2H), 8.00 – 7.93 (m, 4H), 7.59 – 7.48 (m, 3H), 4.36 (t, *J* = 6.6 Hz, 2H), 3.86 (d, *J* = 2.8 Hz, 2H), 2.35 (t, *J* = 7.4 Hz, 2H), 1.98 – 1.88 (m, 1H), 1.88 – 1.79 (m, 2H), 1.79 – 1.69 (m, 2H), 1.56 – 1.48 (m, 2H), 0.93 (d, *J* = 1.3 Hz, 6H). **^{13}C-NMR** (101 MHz, $CDCl_3$) δ 173.7, 166.2, 155.3, 152.7, 132.2, 131.8, 130.7, 129.3, 123.3, 122.8, 70.6, 65.2, 34.4, 28.6, 27.9, 25.8, 24.9, 19.2. **IR (neat, CM^{-1}) v:** 3040-2874 (W), 1715 (S), 1691 (S), **ESI (+)** Calculated for $[C_{23}H_{28}N_2O_4]^+$ ([M+H]$^+$) 397.2122. Found 397.2133.

(*E/Z*)-6-((4-(phenyldiazenyl)benzoyl)oxy)hexanoic acid (8). Orange solid, *E/Z* >90, 75%

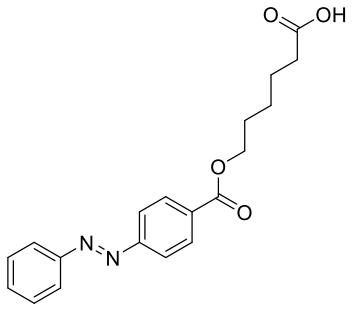

yield. **^{1}H-NMR** (400 MHz, $CDCl_3$) δ 8.21 – 8.15 (m, 2H), 7.99 – 7.92 (m, 5H), 7.58 – 7.48 (m, 3H), 4.37 (t, *J* = 6.6 Hz, 2H), 2.43 (t, *J* = 7.4 Hz, 2H), 1.88 – 1.80 (m, 2H), 1.80 – 1.71 (m, 2H), 1.60 – 1.49 (m, 2H).**^{13}C-NMR** (101 MHz, $CDCl_3$) δ 178.9, 166.2, 155.3, 152.7, 132.2, 131.9, 130.7, 129.3, 123.3, 122.8, 65.1, 33.8, 28.6, 25.7, 24.5. **IR (neat, CM-1) v:** 3040-2874 (W), 1715 (S), 1691 (S), **ESI (+)** Calculated for $[C_{19}H_{21}N_2O_4]^+$ ([M+H]$^+$) 341.1496, found 341.1497.

6-oxo-6-((2-oxohexahydro-4*H*-benzo[*d*][1,3]dioxin-8-yl)oxy)hexyl(*E/Z*)-4(phenyldiazenyl)-benzoate (M2). Orange liquid, *E/Z* >90, 60% yield. **^{1}H-NMR** (400 MHz, $CDCl_3$) δ 8.23 – 8.13 (m, 2H), 7.99 – 7.88 (m, 4H), 7.59 – 7.45 (m, 3H), 4.52 (t, *J* = 3.8 Hz, 1H), 4.45 (dd, *J* = 11.1, 3.8 Hz, 1H), 4.36 (t, *J* = 6.5 Hz, 2H), 4.22 (dd, *J* = 11.1, 2.8 Hz, 1H), 2.38 (t, *J* = 7.5 Hz, 2H), 2.27 – 2.12 (m, 1H), 1.89 – 1.75 (m, 4H), 1.79 – 1.68 (m, 4H), 1.70 – 1.59 (m, 5H), 1.57 – 1.45 (m, 2H).**^{13}C-NMR** (101 MHz, $CDCl_3$) δ 172.1, 166.1, 155.2, 152.6, 147.5, 132.0, 131.8, 130.6, 129.2, 123.2, 122.7, 76.2, 71.9, 68.6, 65.0, 34.2, 28.7, 28.4, 25.6, 24.7, 24.6, 22.5, 18.6. **IR (neat, CM^{-1}) v:** 2939-2866 (W), 1753 (S), 1715 (S). **ESI (+)** Calculated for $[C_{21}H_{21}N_2O_5]^+$ ([M+Na]$^+$) 517,1944. Found 517,1945.

8.5 General procedure for the ROP of functionalized cyclic carbonates

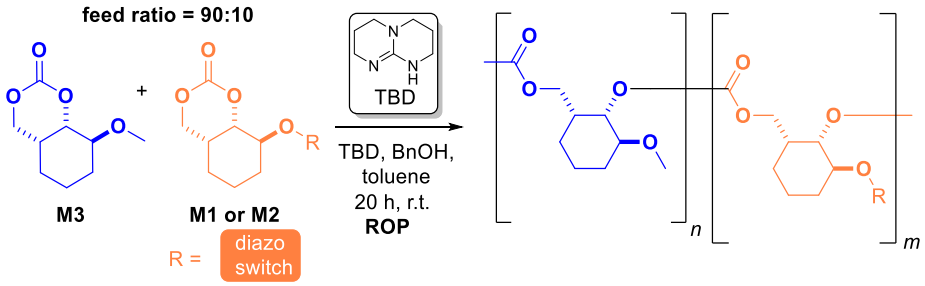

In a nitrogen filled glovebox, a vial equipped with a magnetic stirring bar was charged with the **M1/M2** (0.1 equiv.) and **M3** (1.0 equiv.), followed by a benzyl alcohol (59.2 mM stock solution in toluene, 1.0 mol%) and TBD (29.5 mM stock solution in toluene, 1 mol%). The resulting homogeneous solution was stirred for 20 h at 40 °C. Then, the reaction mixture was quenched with 1 M HCl and a sample was analyzed by ^{1}H-NMR ($CDCl_3$) to determine the conversion. Precipitation from CH_2Cl_2/MeOH provided the purified polymer product, which was collected by filtration and dried in a vacuum drying oven at 40 °C for three days following ^{1}H, ^{13}C and ^{2}D NMR, IR, SEC, and in some cases TGA and DSC analysis[31].

Polymer 1: Orange solid. **^{1}H-NMR** (400 MHz, $CDCl_3$) δ 8.2 – 8.2 (m, 2H), 8.0 – 7.9 (m, 4H),

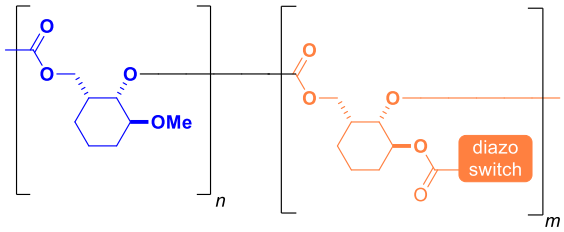

7.6 – 7.5 (m, 3H), 7.5 – 7.3 (m, 5H), 5.2 (s, 1H), 4.9 (s, 1H), 4.4 – 3.7 (m, 2H), 3.5 (s, 1H), 3.4 (s, 3H), 2.3 (s, 1H), 1.9 – 1.3 (m, 8H).**^{13}C-NMR** (126 MHz, CDCl3) δ 187.0, 172.5, 171.9, 171.6, 169.9, 149.1, 148.1, 146.5, 146.0, 140.5, 140.0, 138.1, 96.4, 92.6, 92.4, 90.5, 85.6, 74.1, 73.7, 54.3, 52.4, 47.0, 43.6, 42.2, 40.3, 38.5, 38.2, 36.5, 36.1, 29.3, 18.3. **IR (neat, CM^{-1}) v:** 2933-2823 (W), 1740 (S), **SEC:** 3,51 kg/mol, ***Đ*:** 1,21.

Polymer 2: Orange solid. **^{1}H-NMR** (400 MHz, $CDCl_3$) δ 8.22 – 8.15 (m, 2H), 7.98 – 7.92 (m,

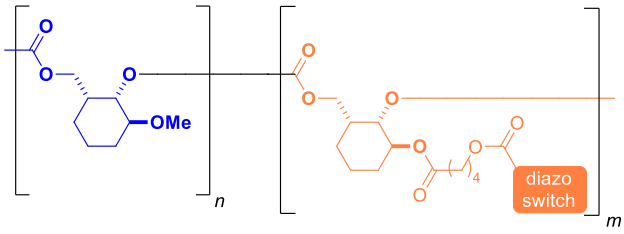

4H), 7.56 – 7.50 (m, 3H), 7.39 – 7.35 (m, 5H), 5.14 (s, 5H), 4.86 (s, 1H), 4.35 (s, 1H), 4.23 – 3.83 (m, 2H), 3.49 (s, 1H), 3.37 (s, 3H), 2.42 – 2.20 (m, 1H), 1.88 – 1.66 (m, 2H), 1.66 – 1.45 (m, 4H), 1.45 – 1.30 (m, 2H).**^{13}C-NMR** (126 MHz, $CDCl_3$) δ 154.8, 152.7, 131.8, 130.7, 129.3, 129.0, 123.3, 122.8, 120.9, 75.2, 73.4, 65.2, 56.9, 56.9, 42.6, 35.2, 29.8, 28.6, 25.1, 23.1, 18.9. **IR (neat, CM^{-1})** *v* **=**2934-2825 (W), 1740 (S), **SEC:** 2,29 kg/mol, ***Đ*:** 1,41.

9. Acknowledgements

This year has been a special one. I experienced significant personal growth, learned a great deal, and made many new friends. This master's degree has had a profound impact on my personal life, professional development, and future career.

First and foremost, I would like to thank Prof. Arjan W. Kleij and Dr. José A. Berrocal for their guidance throughout this research project. I have learned so much from them and am truly grateful for their support and encouragement. Their expertise and feedback helped me perform to the best of my abilities. I also want to thank both research groups for their support and for the many insightful discussions about chemistry and life. In particular, Dr. Stephanie Amos and Dr. Thirusangu M. Senthamarai Ganapathy, who helped me in every aspect of my work and taught me many new techniques and protocols.

I extend my gratitude to my family. Without their support, it would have been impossible to perform at this level. Especially Leon Vermeer, who always stood by me and supported me, showed me the possibilities and broadened my vision. I am also grateful to Roos Wolfs, who was always there for me through good times and bad, offering daily support.

Lastly, I want to thank my triathlon friend and coach. They played a key role in shaping the person I am today. They constantly pushed me to become the best version of myself and always take a step further. Also, Volkert Dekkers, with whom I cycled several times a week, those rides helped me clear my mind after long hours in the laboratory and at university.

10. References

[1] Nunes, L. J. R. The Rising Threat of Atmospheric CO_2: A Review on the Causes, Impacts, and Mitigation Strategies. *Environments*, **2023**, *10*, 66.

[2] Hansen, J. E.; Sato, M.; Lacis, A.; Ruedy, R.; Tegen, I.; Matthews, E. Climate Forcings in the Industrial. Era. *Proc. Natl. Acad. Sci. USA* **1998**, *95*, 12753-12758.

[3] Heede, R. Tracing Anthropogenic Carbon Dioxide and Methane Emissions to Fossil Fuel and Cement Producers, 1854-2010. *Clim. Change* **2014**, *122*, 229-241.

[4] Cox, P. M.; Betts, R. A.; Betts, A.; Jones, C. D.; Spall, S. A.; Totterdell, I. J. Modelling Vegetation and the Carbon Cycle as Interactive Elements of the Climate System. *Int. Geophys.* **2002**, *83*, 259-279.

[5] Xu, J.; Grumbine, R. E.; Shrestha, A.; Eriksson, M.; Yang, X.; Wang, Y.; Wilkes, A. The Melting Himalayas: Cascading Effects of Climate Change on Water, Biodiversity, and Livelihoods. *Conserv. Biol.* **2009**, *23*, 520-530.

[6] Liu, Q.; Wu, L.; Jackstell, R.; Beller, M. Using Carbon Dioxide as a Building Block in Organic Synthesis. *Nat. Commun.* **2015***, 6*, 5933.

[7] Zhang, Z.; Ye, J. H.; Ju, T.; Liao, L. L.; Huang, H.; Gui, Y. Y.; Zhou, W. J.; Yu, D. G. Visible-Light-Driven Catalytic Reductive Carboxylation with CO_2. *ACS Catal.* **2020**, *10*, 10871-10885.

[8] Limburg, B.; Cristòfol, À.; Monica, F. Della; Kleij, A. W. Unlocking the Potential of Substrate-Directed CO_2 Activation and Conversion: Pushing the Boundaries of Catalytic Cyclic Carbonate and Carbamate Formation. *ChemSusChem* **2020**, *13*, 6056-6065.

[9] Grignard, B.; Gennen, S.; Jérôme, C.; Kleij, A. W.; Detrembleur, C. Advances in the Use of CO_2 as a Renewable Feedstock for the Synthesis of Polymers. *Chem. Soc. Rev.* **2019**, *48*, 4466-4514.

[10] Qiao, C.; Shi, W.; Brandolese, A.; Benet-Buchholz, J.; Escudero-Adán, E. C.; Kleij, A. W. A Novel Catalytic Route to Polymerizable Bicyclic Cyclic Carbonate Monomers from Carbon Dioxide. *Angew. Chem. Int. Ed.* **2022**, *134*, e202205053.

[11] Artham, T.; Doble, M. Biodegradation of Aliphatic and Aromatic Polycarbonates. *Macromol. Biosci.* **2008**, *8*, 14-24.

[12] Amass, W.; Amass, A.; Tighe, B. A Review of Biodegradable Polymers: Uses, Current Developments in the Synthesis and Characterization of Biodegradable Polyesters, Blends of Biodegradable Polymers and Recent Advances in Biodegradation Studies. *Polym. Int.* **1998**, *47*, 89-144.

[13] Chen, W.; Meng, F.; Cheng, R.; Deng, C.; Feijen, J.; Zhong, Z. Advanced Drug and Gene Delivery Systems Based on Functional Biodegradable Polycarbonates and Copolymers. *J. Control Release* **2014**, *190*, 398-414.

[14] Huang, J.; Shen, B. Study on Enzymatic Degradation Behavior and Mechanisms in CO_2-Based Polycarbonates with Different Structures. *React. Funct. Polym.* **2025**, *214*, 106339.

[15] Huang, R.; Rintjema, J.; González-Fabra, J.; Martín, E.; Escudero-Adán, E. C.; Bo, C.; Urakawa, A.; Kleij, A. W. Deciphering Key Intermediates in the Transformation of Carbon Dioxide into Heterocyclic Products. *Nat. Catal.* **2019**, *2*, 62-70.

[16] Maquilón, C.; Limburg, B.; Laserna, V.; Garay-Ruiz, D.; González-Fabra, J.; Bo, C.; Martínez Belmonte, M.; Escudero-Adán, E. C.; Kleij, A. W. Effect of an $Al^{(III)}$ Complex on the Regio-and Stereoisomeric Formation of Bicyclic Organic Carbonates. *Organometallics* **2020**, *39*, 1642–1651.

[17] Haba, O.; Tomizuka, H.; Endo, T. Anionic Ring-Opening Polymerization of Methyl 4,6-O-Benzylidene-2,3- Ocarbonyl-a-D-Glucopyranoside: A First Example of Anionic Ring-Opening Polymerization of Five-Membered Cyclic Carbonate without Elimination of CO_2. *Macromol.* **2005**, *38*, 3562-3563.

[18] Nemoto, N.; Sanda, F.; Endo, T. Cationic Ring-Opening Polymerization of Six-Membered Cyclic Carbonates with Ester Groups. *J. Polym. Sci. A Polym. Chem.* **2001**, *39*, 1305-1317.

[19] Kricheldorf, H. R.; Stricker, A. Polymers of Carbonic Acid, 28. $SnOct_2$-Initiated Polymerizations of Trimethylene Carbonate (TMC, 1,3-Dioxanone-2). *Macromol. Chem. Phys.* **2000**, *201*, 2557-2565.

[20] Nederberg, F.; Lohmeijer, B. G. G.; Leibfarth, F.; Pratt, R. C.; Choi, J.; Dove, A. P.; Waymouth, R. M.; Hedrick, J. L. Organocatalytic Ring Opening Polymerization of Trimethylene Carbonate. *Biomacromolecules* **2007**, *8*, 153-160.

[21] Baki, Z. A.; Dib, H.; Sahin, T. Overview: Polycarbonates via Ring-Opening Polymerization, Differences between Six- and Five-Membered Cyclic Carbonates: Inspiration for Green Alternatives. *Polymers* **2022,** *14*, 2031.

[22] G. S. Hartley. The Cis-Form of Azobenzene. *Nat.* **1937**, *140*, 281-281.

[23] Weis, P.; Tian, W.; Wu, S. Photoinduced Liquefaction of Azobenzene-Containing Polymers. *Chem. Eur. J.* **2018**, *24*, 6494-6505.

[24] Xu, W.; Sun, S.; Wu, S. Photoinduzierte, Reversible Fest-flüssig-Übergänge Unter Verwendung Photoschaltbarer Materialien. *Angew. Chem.* **2019**, *131*, 9814–9843.

[25] Birnbaum, P. P.; Linford, J. H.; Style, D. W. G. The absorption spectra of azobenzene and some derivatives. *Trans. Faraday Soc.* **1953***, 49,* 735-74.

[26] Konieczkowska, J.; Siwy, M. Comprehensive Investigations of trans-cis-trans Isomerization in the Solid State for Azo Polyimides. *Dyes Pigm*. **2023,** *219*, 111558.

[27] Kim, D. Y.; Li, L.; Jiang, X. L.; Shivshankar, V.; Kumar, J.; Tripathy, S. K. Polarized Laser Induced Holographic Surface Relief Gratings on Polymer Films. *Macromolecules*. **1995**, *28*, 8835-8839.

[28] Deng, Y.; Li, N.; He, Y.; Wang, X. Hybrid Colloids Composed of Two Amphiphilic Azo Polymers: Fabrication, Characterization, and Photoresponsive Properties. *Macromolecules* **2007**, *40*, 6669-6678.

[29] Zhou, H.; Xue, C.; Weis, P.; Suzuki, Y.; Huang, S.; Koynov, K.; Auernhammer, G. K.; Berger, R.; Butt, H. J.; Wu, S. Photoswitching of Glass Transition Temperatures of Azobenzene-Containing Polymers Induces Reversible Solid-to-Liquid Transitions. *Nat. Chem*. **2017**, *9*, 145-151.

[30] Bond, C. W.; Cresswell, A. J.; Davies, S. G.; Fletcher, A. M.; Kurosawa, W.; Lee, J. A.; Roberts, P. M.; Russell, A. J.; Smith, A. D.; Thomson, J. E. Ammonium-Directed Oxidation of Cyclic Allylic and Homoallylic Amines. *J. Org. Chem*. **2009**, *74*, 6735-6748.

[31] Shi, W.; Senthamarai, T.; Lanzi, M.; Orlando, P.; Nogués Martín, R.; Kleij, A. W. Access to Highly Functional and Polymerizable Carbonate-Drug Conjugates. *ChemSusChem* **2025**, *18*, e202500031.

[32] Lutjen, A. B.; Quirk, M. A.; Barbera, A. M.; Kolonko, E. M. Synthesis of (E)-Cinnamyl Ester Derivatives via a Greener Steglich Esterification. *Bioorg. Med. Chem*. **2018**, *26*, 5291-5298.

[33] Jordan, A.; Whymark, K. D.; Sydenham, J.; Sneddon, H. F. A Solvent-Reagent Selection Guide for Steglich-Type Esterification of Carboxylic Acids. *Green Chem*. **2021**, *23*, 6405-6413.

[34] Bandara, H. M. D.; Burdette, S. C. Photoisomerization in Different Classes of Azobenzene. *Chem. Soc. Rev.* **2012**, *41*, 1809-1825.

[35] Moniruzzaman, M.; Talbot, J. D. R.; Sabey, C. J.; Fernando, G. F. The Use of ^{1}H-NMR and UV-Vis Measurements for Quantitative Determination of *trans*/*cis* Isomerization of a Photo-Responsive Monomer and Its Copolymer. *J. Appl. Polym. Sci*. **2006**, *100*, 1103-1112.

[36] Robert, T.; Henrard, G.; Tassignon, B.; Serez, A.; De Winter, J.; Dugourd, P.; Cornil, J.; Chirot, F.; Gerbaux, P. Back Isomerization Kinetics of Molecular Photoswitches: Complementary Insights from Liquid Chromatography and Ion Mobility Measurements. *Anal. Chem*. **2025**, 97, 9405-9413.

[37] Axelrod, S.; Shakhnovich, E.; Gómez-Bombarelli, R. Thermal Half-Lives of Azobenzene Derivatives: Virtual Screening Based on Intersystem Crossing Using a Machine Learning Potential. *ACS Cent. Sci.* **2023**, *9*, 166-176.

[38] Moriehima, Y.; Tsuji, M.; Seki, M.; Kamachi', M. Synthesis, NMR Relaxation, and Photoisomerization of Amphiphilic Polyelectrolytes Covalently Tethered with Azobenzene Moieties Having Bulky Hydrophobic Substituents. *Macromolecules* **1993**, *26*, 3299-3305.

[39] Imato, K.; Kaneda, N.; Ooyama, Y. Recent Progress in Photoinduced Transitions between the Solid, Glass, and Liquid States Based on Molecular Photoswitches. *Polym. J.* **2024**, *56*, 269-282.

[40] Dong, M.; Babalhavaeji, A.; Samanta, S.; Beharry, A. A.; Woolley, G. A. Red-Shifting Azobenzene Photoswitches for in Vivo Use. *Acc. Chem. Res.* **2015**, *48*, 2662-2670.

[41] Zhou, Y.; Chen, M.; Ban, Q.; Zhang, Z.; Shuang, S.; Koynov, K.; Butt, H. J.; Kong, J.; Wu, S. Light-Switchable Polymer Adhesive Based on Photoinduced Reversible Solid-to-Liquid Transitions. *ACS Macro. Lett.* **2019**, *8*, 968-972.

[42] Wu, S.; Wang, L.; Kroeger, A.; Wu, Y.; Zhang, Q.; Bubeck, C. Block Copolymers of PS-b-PEO Co-Assembled with Azobenzene-Containing Homopolymers and Their Photoresponsive Properties. *Soft Matter* **2011**, *7*, 11535-11545.

[43] Sardar, J.; Mäeorg, U.; Krasnou, I.; Baddam, V.; Gudkova, V.; Krumme, A.; Savest, N.; Tarasova, E.; Viirsalu, M. Synthesis of Polymerizable Ionic Liquid Monomer and Its Characterization. *Mater. Eng. Res.* **2016**, *111*, 012021.

[44] Kazemi, M.; Noori, Z.; Kohzadi, H.; Sayadi, M.; Kazemi, A. A Mild and Efficient Procedure for the Synthesis of Ethers from Various Alkyl Halides. *Iran. Chem. Commun.* **2013**, *1*, 43-50.

[45] Ohtani, N.; Ohta, T.; Hosoda, Y.; Yamashita, T. Phase Behavior and Phase-Transfer Catalysis of Tetrabutylammonium Salts. Interface-Mediated Catalysis. *Langmuir* **2004**, *20*, 409-415.

[46] Elizabeth M. Sanford, Christina C. Lis, and Nikolas R. Mc Pherso. The Preparation of Allyl Phenyl Ether and 2-Allylphenol the Williamson Ether Synthesis and Claisen Rearrangement. *J. Chem. Educ.* **2009**, *86*, 1422.

[47] Larock, R. C.; Leach, D. R. Organopalladium Approaches to Prostaglandins. 3. Synthesis of Bicyclic and Tricyclic 7-Oxaprostaglandin Endoperoxide Analogues via Oxypalladation of Norbornadiene. *J. Org. Chem.* **1984**, *49*, 2144-2148.

[48] Wells, G. J.; Tao, M.; Josef, K. A.; Bihovsky, R. 1,2-Benzothiazine 1,1-Dioxide P2-P3 Peptide Mimetic Aldehyde Calpain I Inhibitors. *J. Med. Chem.* **2001**, *44*, 3488-3503.

[49] Yue, Y.; Norikane, Y.; Azumi, R.; Koyama, E. Light-Induced Mechanical Response in Crosslinked Liquid-Crystalline Polymers with Photoswitchable Glass Transition Temperatures. *Nat. Commun.* **2018**, *9*, 3234.

[50] Ishiba, K.; Morikawa, M. A.; Chikara, C.; Yamada, T.; Iwase, K.; Kawakita, M.; Kimizuka, N. Photoliquefiable Ionic Crystals: A Phase Crossover Approach for Photon Energy Storage Materials with Functional Multiplicity. *Angew. Chem. Int. Ed.* **2015**, *54*, 1532-1536.

[51] Ni, J.; Lanzi, M.; Lamparelli, D. H.; Kleij, A. W. Ring-Opening Polymerization of Functionalized Aliphatic Bicyclic Carbonates. *Polym. Chem.* **2023**, *14*, 4748-4753.

[52] Arya, P.; Jelken, J.; Lomadze, N.; Santer, S.; Bekir, M. Kinetics of Photo-Isomerization of Azobenzene Containing Surfactants. *J. Chem. Phys.* **2020**, *152*, 024904.